Final Draft
of the original manuscript:

Olivieri, L.; Tena, A.; de Angelis, M.G.; Hernandez Gimenez, A.; Lozano, A.E.; Sarti, G.C.:

Sorption and transport of CO2 in copolymers containing soft (PEO, PPO) and hard (BKDA-ODA and BPDA-ODA) segments at different temperatures: Experimental data and modeling

In: Journal of Membrane Science (2016) Elsevier

DOI: 10.1016/j.memsci.2016.07.057

Sorption and transport of CO_2 in copolymers containing soft (PEO, PPO) and hard (BKDA-ODA and BPDA-ODA) segments at different temperatures: experimental data and modeling

Luca Olivieri,[(1)] Alberto Tena,[(2)I] Maria Grazia De Angelis[(1)II], Antonio Hernández Giménez,[(2)] Angel E. Lozano,[(2,3)] Giulio Cesare Sarti[(1)].

(1) Dipartimento di Ingegneria Civile Chimica Ambientale e dei Materiali, Alma Mater Studiorum-Università di Bologna, Via Terracini 28, Bologna, Italy

(2) SMAP UA UVA-CSIC, Universidad de Valladolid, Facultad de Ciencias, Real de Burgos s/n, 47071 Valladolid, Spain

(3) Instituto de Ciencia y Tecnología de Polímeros, CSIC, Juan de la Cierva 3, 28006 Madrid, Spain

Abstract

In this work, we studied CO_2 sorption and transport in two series of aliphatic-aromatic copolyimide membranes, as a function of chemical formulation, pressure and temperature. Such materials are formed by two distinct phases with rather different properties: the first one is formed of rubbery polyether segments (poly (propylene oxide) (PPO) or poly(ethylene oxide) (PEO)), characterized by favorable energetic interactions with CO_2 and high flexibility, which endows the copolymers with high CO_2 permeability, suitable for capture processes. The second phase is formed by hard glassy polyimide blocks, randomly distributed at the microscopic level, which provide the necessary thermal, chemical and mechanical stability.

Previous studies indicate that CO_2 permeability increases with increasing the amount of polyether phase in the copolymers; in the present work we investigate more deeply the interactions and synergies occurring between the two phases, by focusing separately on the CO_2 solubility and diffusivity terms that contribute to permeability.

In particular, by studying the shape of the solubility isotherm, as well as the values of diffusivity, sorption enthalpy and activation energy, we were able to monitor the transition from a glassy-like to a rubbery-like behavior as the fraction of rubbery component in the copolymer increases. The data indicate that polyether enhances CO_2 permeability by acting mostly on diffusivity, while the solubility contribution is less affected on a quantitative basis. However, the qualitative behavior of solubility allows understanding the nature of interactions between the two phases. In particular, by using a simple additive approach to estimate the CO_2 solubility of the copolymer, and the Non Equilibrium Lattice Fluid (NELF) to evaluate the CO_2 solubility in the pure homopolymers, one concludes that the copolymers sorption behavior is “ideal”, i.e. purely additive, indicating a good combination of the two phases. The copolymer volume, on the other hand, shows a contraction upon combination of the two phases. The NELF modeling of solubility data allows attributing such a contraction only to the glassy phase, whose excess free volume is reduced in the presence of the rubbery portion in the copolymer, which possibly partly occupies such excess volume, indicating a strong interpenetration of the two phases.

[I] Present Address: Helmholtz-Zentrum Geesthacht, Institute of Polymer Research, Max-Planck-Str.1, 21502 Geesthacht, Germany

[II] Corresponding author. E-mail: grazia.deangelis@unibo.it

Introduction

Carbon dioxide capture from gaseous streams, like flue gas, natural gas, biogas, syngas, is emerging as a crucial process in energy production for both economical and environmental reasons. In this framework, the development of a highly efficient and economic process for CO_2 removal is required[1]. The separation of CO_2 can be achieved by traditional processes, like amine-based absorption or physical adsorption on porous solids, which require high capital cost for large volume columns and high operative costs for energy consumption during regeneration. Those are some of the motivations that drive interest of researchers to study the membrane-based removal of CO_2 from gas mixtures [2,3].

In a membrane separation process, it is important to have a membrane that guarantees high flux of the more permeable component and high separation factor that correspond to high values of permeability and selectivity, respectively. It is well known, however, that, given a certain value of permeability, there is a maximum selectivity that can be achieved with polymeric membranes, and vice versa, according to an upper bound drawn by Robeson for existing polymeric materials [4].

Usually, due to their rigid structure, glassy polymers and in particular polyimides show good mechanical, thermal and chemical resistance but modest permeability [5]. On the contrary, high permeability values can be observed in many rubbery polymers due to the flexibility of polymeric chains, although such properties are usually accompanied by low thermo- and chemical resistance.

According to the previous considerations, therefore, a possible solution could rely on the design of copolymers formed by rubbery and glassy domains, in which the properties can be optimized by a careful choice of the type and amount of different monomers.

In this study we focused on the characterization of two series of co(polyether-imide)s, i.e. block copolymers forms by a glassy polyimide and a rubbery polyether. In particular, the materials studied in this work are characterized by two different couples of polyimide and polyether segments. The first type is obtained by reaction of 3,3’,4,4′-biphenyltetracarboxyilic dianhydride

(BPDA) with a mixture of 4,4'-oxydianiline (ODA) and bis(2-aminopropyl) poly(propylene oxide) (PPO) with nominal molecular weight of 4000 g/mol. (BPDA-PPO4000-ODA). The second set is obtained by combining 3,3',4,4'- benzophenone tetracarboxylic dianhydride (BKDA) with a mixture of the diamines 4-4'-oxydianiline (ODA) and α,ω-diamine poly(ethylene oxide) (PEO) with nominal molecular weight of 6000 g/mol (BKDA-PEO6000-ODA).

Previous experimental works indicate that the CO_2 permeability and selectivity of such materials increase by increasing the amount of polyether rubbery phase [6-10]. Such component has flexible chains, which can guarantee high CO_2 permeability, due to their mobile structure coupled with a high affinity towards CO_2. Such increase may be due partly to contribution of diffusivity, because of the greater flexibility of the rubbery chains with respect to the glassy ones, but also due to a contribution of higher solubility of CO_2 in the polar polyether rubbery phase owing to its interaction with the oxygen atom of the ether moieties[11-12]. In these materials it was found that the permeability of the different gases follows the sequence: $P_{CO_2} > P_{CH_4} > P_{O_2} > P_{N_2}$ [6-10] which is the order of decreasing penetrant condensability; moreover, the diffusion coefficient is only a weak function of penetrant size, because of their poor polymer-size sieving ability. Therefore, the relative permeability of each penetrant is largely determined by its solubility.

There are also indications that soft and hard blocks in those copolymers form a micro-segregated structure, with a rubbery and glassy phase that are not completely independent, but interact to some extent [6-10]. As it was demonstrated in other papers [6,7], T_g of the polyether is normally between -80 and -60 °C, i.e. well below the temperature of common permeability measurement, and T_g of the aromatic polyimide is normally between 200 and 270 °C, i.e. well above the measurement temperature; thus there is good separation between the two phases because two different T_g values are detected. In particular with DSC analysis for BPDA-PPO-ODA 1/1 and BPDA-PPO-ODA 2/1 it was possible to detect glass transition temperature for both phases, while for BKDA-PEO-ODA

copolymers it was possible to detect the aromatic phase T_g only. No specific morphology was observed in the copolymers, and thus we can consider that they are randomly distributed.

For such reasons, given the encouraging permeability results [6-10], we decided to study in more detail the sorption and diffusion mechanisms that govern permeation, studying the effect that the amount of rubbery phase has on the two separate contributions, i.e. solubility and diffusivity. We also tested the effect of temperature, in the range between 30 and 60°C. Such analysis allows evaluating the sorption enthalpy and activation energy of diffusion, and find their dependence on copolymer formulation. Such analysis provides a further insight into the degree of interaction between phases and also on the dominating nature of the final copolymer, because such values are usually different for rubbery and glassy polymers.

Finally, the data obtained were modeled in order to understand the mechanisms governing the interactions between the two phases from their behavior. The modeling work was carried out only on the sorption data, while the diffusion coefficients were estimated and treated as effective values representative of the overall composite structure. A more rigorous approach, involving the separate contributions of diffusion in the two phases, would require a detailed knowledge of their spatial distribution, that is very difficult to determine and beyond the scope of the present work.

We assumed, for the purposes of modeling, that the two phases are randomly distributed, and thus that the sorption of the system can be treated as the one of a composite material where the properties of the composite are a fairly simple combination of the properties of the two phases.

However, one has to consider that such copolymers are formed by two domains that are chemically and physically rather different, in particular one is rubbery and the other one is glassy. Those two states have a different thermodynamic behavior, and the solubility in such structures must be treated with specific modeling tools [13]. The rubbery phase is in true thermodynamic equilibrium and its density can be calculated from an Equation of State (EoS) once temperature and pressure are fixed; for the gas-rubbery polymer mixture that is formed as the result of the sorption process, the state is

completely specified by temperature, pressure and composition (or temperature, pressure and density). The solubility isotherms of gases in rubbery polymers can be linear, or concave to the concentration axis when sorption-induced swelling becomes relevant, as in the case of CO_2 sorption. The sorption in such phase can be modeled with an approach suitable for macromolecular structures, either using the activity coefficient approach, like the Flory Huggins (FH) model [14-16], or the Equation of State approach, as the Lattice Fluid [17], SAFT or [18] PHSC model [19]. Usually, EoS models contain a limited number of adjustable parameter, only one of them is a binary mixture parameter while the others are pure component parameters whose values are obtained directly from the pure polymer or pure penetrant behaviors; in addition EoS models allow predicting, without additional input, the density of the gas-polymer matrix, i.e. the swelling of the polymer induced by gas sorption, that is not possible using an activity coefficient model [20].

The glassy phase is in a pseudoequilibrium state where mobility is hindered and its density has a value lower than at equilibrium, which depends on the system history. Typically, the gas solubility isotherm in an amorphous glassy polymer can be linear, as in the case of light gases, or concave to the pressure axis: the larger is the out of equilibrium degree of the matrix, i.e. its excess free volume, the more marked is the deviation from linear behavior in the low pressure range. In some particular cases, like the absorption of alcohols in high free volume glassy polymers, the isotherm exhibits even a sigmoidal shape [21].

One of the most commonly used approaches to describe gas sorption in glassy polymers is the Dual Mode Sorption model, that combines an Henry's law contribution and a Langmuir term and contains three binary parameters for each gas-polymer mixture and temperature [22-24]. The success of the model lies in its ease of use and possibility to a qualitative link between the three parameters and physical properties of the system.

A different tool, that can be seen as an extension to the glassy state of the EoS model valid for rubbery polymers, is the Non Equilibrium Theory for Glassy Polymers (NET-GP) approach [13, 25-

26]. With respect to the EoS models, such approach adopts an additional state variable to univocally define the state of the glassy systems and of its mixtures, namely the polymer density, which differs from the equilibrium value and must be provided as an input to the model. A non equilibrium version has been proposed for each of the main EoS models for polymers, generating the NE-LF, NE-SAFT, NE-PHSC models, that adopt the same set of parameters proposed by the original theories [13]. As an example: the CO_2 sorption in polysulfone can be described with SAFT EoS above T_g and the NE-SAFT model below T_g with the same, constant values of pure component and binary parameters [13].

It is thus clear that different approaches can be followed to model the CO_2 sorption in the rubbery and glassy part of the copolymers studied. In principle, one can use the FH model for the rubbery phase, and the DMS model for the glassy one, but such theories have no relation one with another. For this reason, in this work, we decided to use EoS models to model the CO_2 sorption in the rubbery part, and the corresponding Non Equilibrium version (NE-EoS) for the glassy phase. Such choice allows us to treat both phases with a unique scheme of representation,i.e. the Lattice Fluid framework in the case we selected of LF models, (as an alternative one could have applied the hard sphere chain picture used in the case of SAFT and PHSC theories) and a homogenous set of parameters. Plus, such choice allows estimating the gas-induced dilation in the rubbery part of the copolymer and to predict the solubility isother in both phases.

The choice of the particular EoS model is based on the physico-chemical nature of the systems investigated: we chose the Lattice Fluid Theory by Sanchez and Lacombe [17] because the substances under study have a mild or negligible polarity, and are not crosslinked. Furthermore, it has been shown in previous works that the LF EoS model is a reliable tool to model the CO_2 sorption in rubbery polymers similar to the ones inspected here, namely the crosslinked polyethylene oxide (XL PEO) [27]; and that the NE-LF model is also successful in representing the sorption of gases and vapors in a glassy polyimide system such as Matrimid [28,29].

Besides, both the LF and NELF models were used by several authors for representing solubility in a wide variety of situations as the sorption of gases, vapors and liquids in amorphous homopolymers, semicrystalline structures [30], mixed matrix membranes, blends, copolymers, and to represent sorption isotherms correctly in all such systems, independent of their shape [13, 31-37].

After having used the chosen models to represent the CO_2 solubility in the two distinct phases, the solubility in the copolymer was calculated by summing the two contributions, according to a simple additive scheme in which each phase behaves like the corresponding pure homopolymer, in terms of pure component and binary gas-polymer parameters. The comparison with experimental data provides a further insight into the extent and nature of interactions between the two phases that form the material and their effect on the CO_2 transport.

To our knowledge, this is probably the first work related to the modeling of a copolymer formed by rubbery and glassy phases, which are segregated at the microscale level. Additional insights in this type of materials could shed light on the design of new materials with enhanced gas separation properties

1. Experimental

1.1. Materials

Four samples of BPDA-PPO4000-ODA copolymers were studied, containing 29.70 wt%, 43.50 wt %, 59.17 wt% and 67.38 wt% of PPO and named as BPDA-PPO-ODA 1/1, 2/1, 4/1, 6/1. The samples BKDA-PEO6000-ODA 2/1 and 4/1 contained respectively 43.80 wt% and 60.40 wt% [7] of PEO. In Fig. 1 chemical structures of PPO, PEO, BPDA, BKDA and ODA are reported. Polymers were synthesized mixing polyether aliphatic diamine with aromatic diamine in appropriate weight ratio (1/1, 2/1, 4/1, 6/1) in N,N’-dimethylacetamide (DMAc). Reaction mixture thus obtained was cooled down to 0°C and dianhydride was added stirring overnight at room temperature to obtain a high viscosity solution, which was diluted in DMAc to the appropriate

viscosity for casting to obtain thin films, to be used for gas separation characterization, which resulted opaque. For more details refer to previous works [6–10].

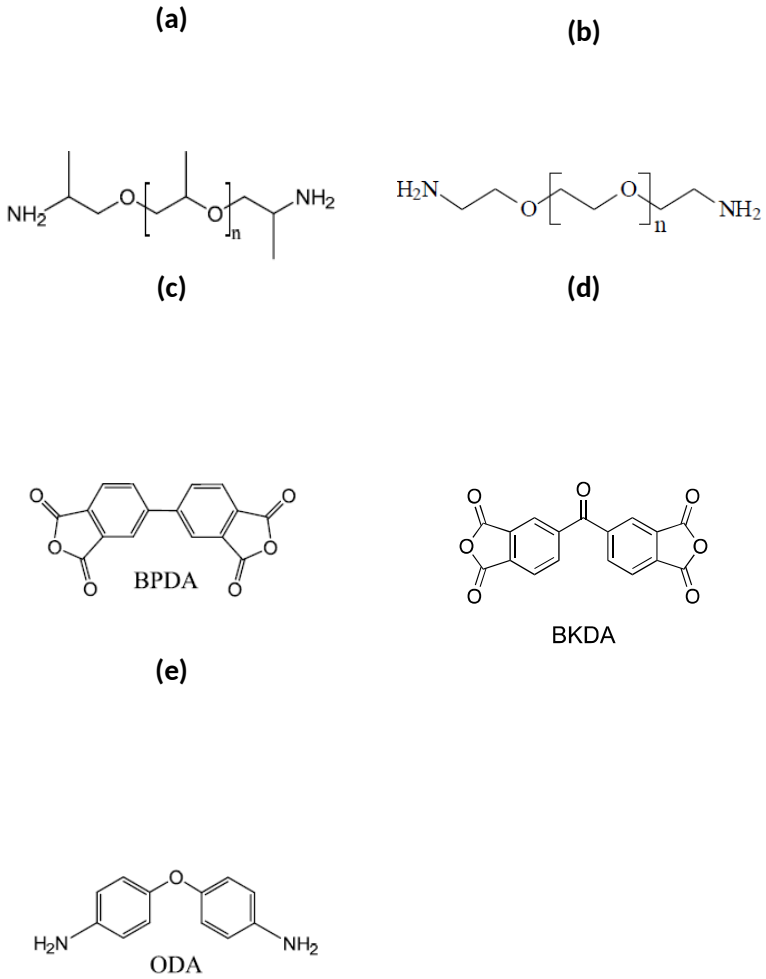

Fig.1: Structure of (a) diamino-terminated PPO, (b) diamino-terminated PEO, (c) BPDA, (d) BKDA and (e) ODA [6,7]

The density of the copolymers inspected varies with the composition: an analysis of the density data can give information on the mixing volume between the two phases forming the copolymer. Densities of PPO-based 1/1 and 2/1 copolymers and of the corresponding homopolymers are known from a previous work [6], while data relative to the PEO-based samples were obtained in this work by measuring the samples weight and volume. For the homopolymers density values, we used literature data [5, 6, 38-41].

The values of specific volume of these samples were plotted versus the mass percentage of rubbery phase, w_R, in Figure 2 and compared with "ideal mixture" volume calculated from the pure rubber and pure glass specific volumes, $\hat{v}_R^0$ and $\hat{v}_G^0$, as follows:

$$\hat{v}_{ideal} = w_R \hat{v}_R^0 + (1 - w_R)\hat{v}_G^0 \quad (1)$$

It can be seen in Figure 2a and 2b that for both types of copolymers, the volume is lower than the ideal mixture value, so that a contraction occurs upon phase mixing. The volume of tested materials can be interpolated with the following equations:

$$\hat{v}_{copol} = 3.54 \cdot 10^{-1} \omega_{PPO}^3 - 3.36 \cdot 10^{-1} \omega_{PPO}^2 + 2.77 \cdot 10^{-1} \omega_{PPO} + 7.32 \cdot 10^{-1} \quad \text{(PPO-based)}$$

(2)

$$\hat{v}_{copol} = 8.31 \cdot 10^{-2} \omega_{PEO}^2 + 7.88 \cdot 10^{-2} \omega_{PEO} + 7.28 \cdot 10^{-1} \quad \text{(PEO-based)}$$

(3)

The negative value of the mixing volume can be due to a contraction of the glassy phase, of the rubbery phase, or both. Usually, glassy polymers have free volume in excess with respect to their equilibrium value, which can vary depending on the preparation protocol and history of the solid material. Moreover, it is known from the study of the properties of semicrystalline polymers, that the density of the rubbery amorphous regions may be lower than that of the equilibrium value when surrounded by crystalline domains, due to the compressive stress applied by such structures [30]. Some previous data indicate that the soft rubbery segments penetrate part of the free volume of the glassy domains in the copolymers here inspected. Therefore, the appearance of a negative mixing volume is not surprising. In the following modeling analysis of CO_2 solubility data, we will investigate in more detail this aspect.

(a) (b)

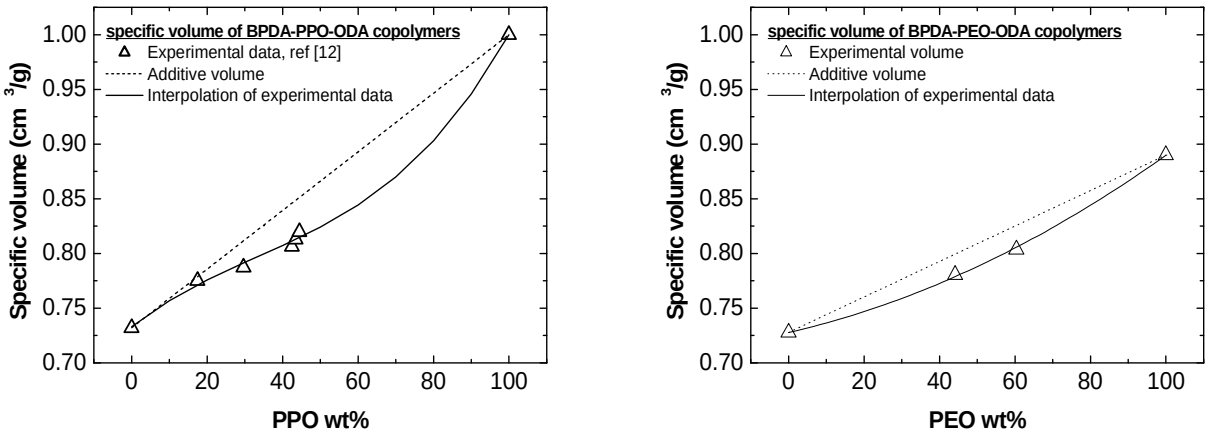

Fig. 2: Specific volumes of (a) BPDA-PPO-ODA and (b) BKDA-PEO-ODA copolymers as a function of rubbery phase weight percentage; solid lines are interpolations (Eq. 2 and eq. 3) and dashed lines is additive rule (Eq. 1). Data for BPDA-PPO-ODA are taken from ref. [6]; data for BKDA-PEO-ODA are measured in this work by measuring the sample weight and volume. Data for pure homopolymers PEO and BKDA-ODA are taken from ref. [38] and [40], respectively.

It has to be noted out that, in PEO-containing materials, depending on thermal treatment and polyether content, there is also some degree of crystallinity, which increases with the amount of PEO. In particular, increasing the content of PEO and the treatment temperature, there is a higher phase segregation, and the separated polyether phase, which becomes pure, can crystallize up to 63% of crystalline PEO/total polymer for a copolymer which contains 69% of PEO treated at 260°C [7,8]. Anyway in a previous study, it was observed that, at 30°C, BKDA-PEO-ODA 2/1 and 4/1, treated at 180°C, contain 0.0% and 0.9% of total PEO in the crystalline state, respectively [6–9]. On the contrary PPO copolymers did not show any crystallization and in particular all the samples were treated at 160°C except sample 1/1 treated at 200°C to be fully imidized.

In Table 1 we report composition, density ρ and thickness l of all tested materials, in particular for BPDA-PPO-ODA 4/1 and 6/1 density has been calculated by means of equation (2):

Table 1: Properties of copolymer samples investigated in this work.

Sample	Rubber content	Amorphous rubber content	ρ	Thickness	Reference for density	Treatment temperature	T_g Rubber	T_g Glass
	wt%	wt%	g/cm^3	μm		°C	°C	°C

BPDA-PPO-ODA 1/1	29.70	29.70	1.267	161±19	Buoyancy method [6]	200	-71.6 [6]	240.1 [6]
BPDA-PPO-ODA 2/1	43.50	43.50	1.210	57±16	Buoyancy method [6]	160	-69.1[6]	225.7 [6]
BPDA-PPO-ODA 4/1	59.17	59.17	1.187	141±8	Interpolated, Equation 2	160	N/A	N/A
BPDA-PPO-ODA 6/1	67.38	67.38	1.159	154±43	Interpolated, Equation 2	160	N/A	N/A
BKDA-PEO-ODA 2/1	43.80	43.80	1.281	116±1	This work, weight and volume measurement	180	N/A	242 [8]
BKDA-PEO-ODA 4/1	60.40	59.90	1.244	107±2	This work, weight and volume measurement	180	N/A	189 [8]

1.2. Experimental: sorption measurements

Sorption experiments were carried out in a pure gas pressure decay apparatus described in previous works [42,43]. At each temperature we carried out two or more experimental tests to verify reliability and reproducibility of experimental results.

Following a well-accepted procedure and monitoring the pressure decay in a known volume we evaluated equilibrium concentration of CO_2 in the polymers at increasing pressures up to 30 bar, obtaining solubility isotherms, and calculating also diffusivity D by fitting the sorption kinetics data of each sorption step with the following equation [44]:

$$\frac{M_t - M_0}{M_\infty - M_0} = 1 - \sum_{n=1}^{\infty} \frac{2\alpha(1+\alpha)}{1+\alpha+\alpha^2 q_n^2} \exp(-Dq_n^2 t/l^2)$$

(4)

M_0 and M_∞ are the initial and final equilibrium mass uptake in the sorption step, respectively, α is the ratio between the volume of gas phase and that of the membrane, corrected for the partition coefficient of gas between the gaseous phase and the polymeric phase, l is the thickness of the membrane, and q_n variables are the positive, nonzero, solutions of the equation: $tg(q_n) = -\alpha q_n$.

Considering data available at different temperatures, sorption enthalpies $\Delta\tilde{H}_S$ and diffusion activation energy E_D can be calculated with the following two equations, where R is the universal gas constant:

$$-\frac{\Delta\tilde{H}_S}{R} = \left(\partial \ln S / \partial (1/T)\right)_p \quad (5)$$

$$-\frac{E_D}{R} = \left(\partial \ln D / \partial (1/T)\right)_{c_{CO_2}} \quad (6)$$

2. Experimental results

2.1. Solubility and diffusivity of CO_2 in BPDA-PPO4000-ODA copolymers

CO_2 sorption experiments were carried out up to 30 bar at 30, 45 and 60°C in BPDA-PPO 4000-ODA copoly(ether-imide)s and solubility and diffusivity were evaluated at various pressures.

The solubility data in each copolymer are reported in Fig. 3 at different temperatures. First of all one can notice that these materials show quite high CO_2 solubility, up to 40 cm^3(STP)/cm^3 at 20 bar, which is similar to the value found for commercial rubbery PDMS that is equal to 28 cm^3(STP)/cm^3 at the same pressure [45].

The solubility, as usual, decreases with increasing temperature and the data can be used to calculate sorption enthalpies, shown in a subsequent section. Interestingly, by increasing the proportion of the rubbery phase in the copolymer, the shape of the trend line that best fits the mean values of solubility changes. In particular, such trend lines are slightly concave to the concentration axis (like in rubbery sorption) if the rubbery phase content is higher than 43 wt% (Fig. 3c, d). If rubbery phase percentage is lower than 30% wt% the trend line that provides the best fitting becomes concave to pressure axis, like in glassy polymers (Fig. 3a).

The diffusivity values, calculated from sorption kinetics data, are reported in Figure 4 for the various copolymers at different temperatures. The extent of CO_2 diffusivity variation with temperature is lower for materials with higher amount of rubbery PPO. The diffusivity observes a step increase of 2 orders of magnitude when the weight percentage of PPO in the sample goes above 44 wt% (from $10^{-8} \div 10^{-7}$ cm^2/s to 10^{-5} cm^2/s). Such a remarkable increase indicates a strong variation of the copolymer nature with increasing amount of PPO, with a dramatic increase of

polymer flexibility above a certain threshold. The solubility behavior, on the other hand, seems less affected by the copolymer formulation, as is discussed above.

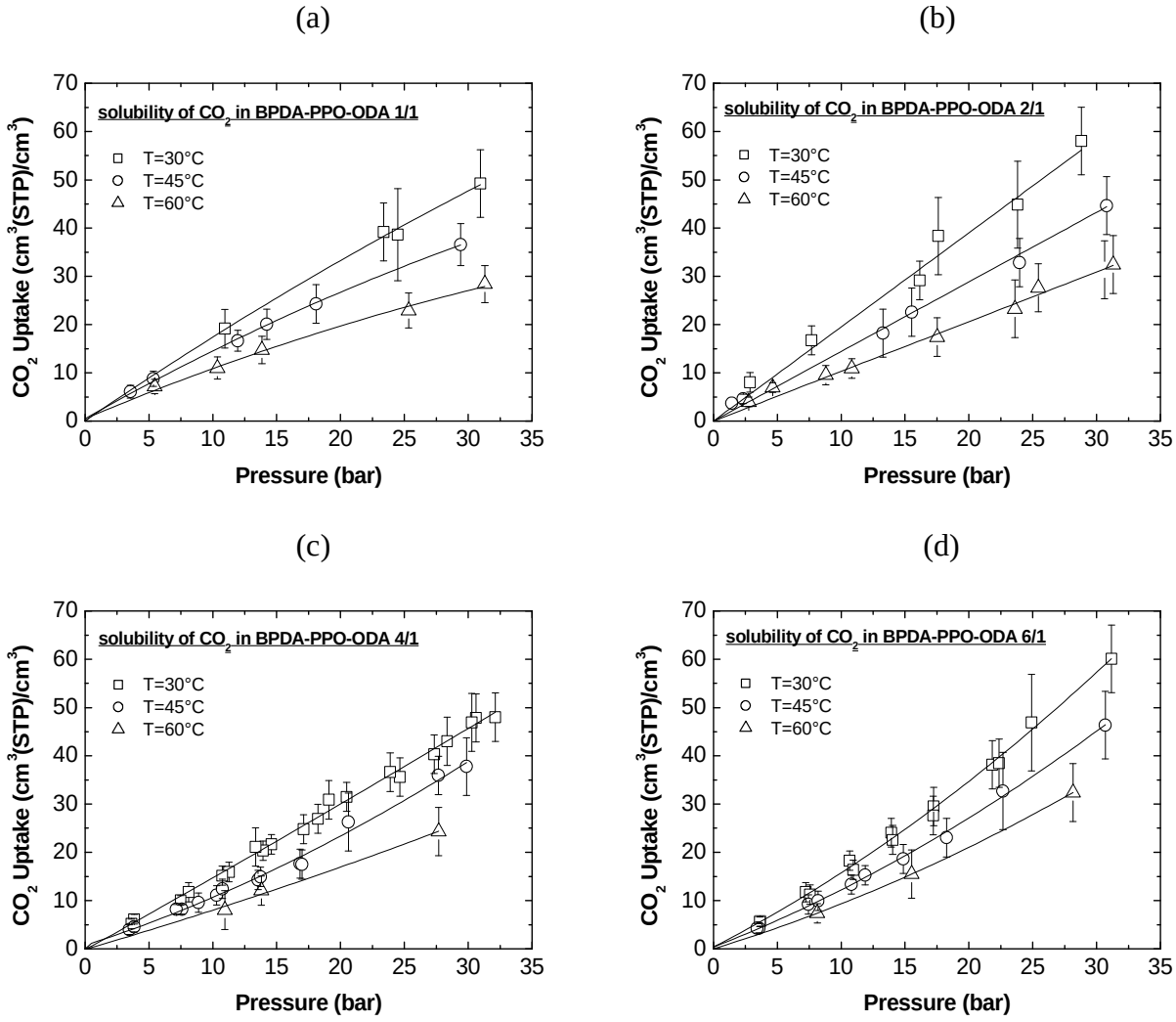

Fig. 3: The effect of temperature on CO_2 solubility isotherms in BPDA-PPO4000-ODA 1/1 (a), 2/1 (b), 4/1 (c) and 6/1 (d) samples. Solid lines are data interpolations.

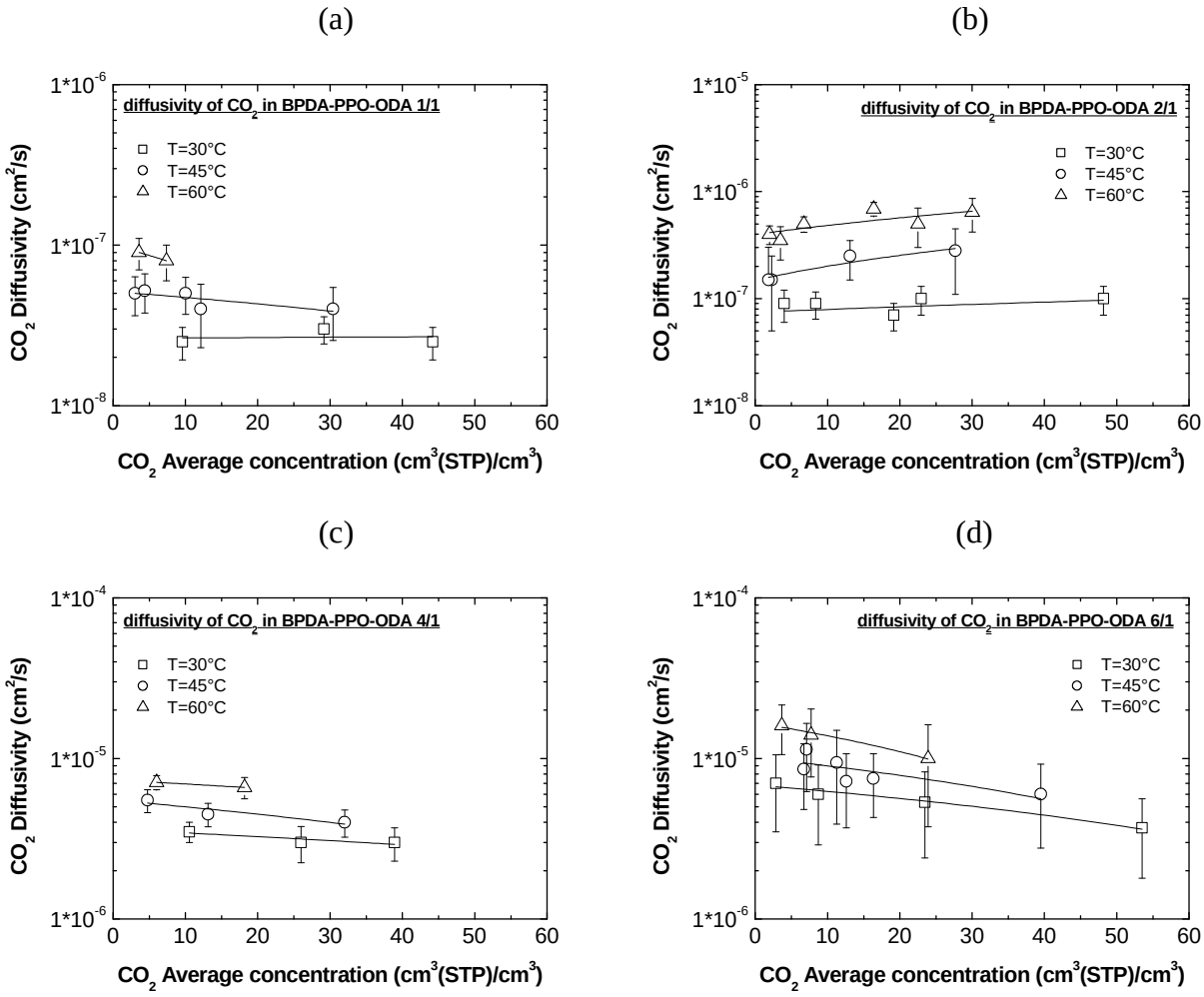

Fig. 4: The effect of temperature on CO_2 diffusivity in BPDA-PPO4000-ODA 1/1 (a), 2/1 (b), 4/1 (c) and 6/1 (d) samples. Solid lines are data interpolations.

The influence of copolymer composition on permeability was studied in previous works [6-10], and showed an enhancement of permeability with increasing PPO content in the membranes. In this work, we have the possibility of analyzing the effect that the copolymer composition has, separately, on diffusivity and solubility contribution.

Solubility of CO_2 is a very weak function of the copolymer composition in the entire range of temperature investigated, as can be seen from Fig. 5 for the temperature of 30°C. Corresponding charts obtained at 45 and 60°C show similar trends and are visible in Fig. S1 and Fig. S2 in the Supplementary Material.

On the other hand, it is evident from Fig. 6 that increasing PPO percentage in the material has a strong effect on CO_2 diffusivity, at 30°C. Diffusivity value for the copolymer 1/1 is one order of

magnitude higher with respect to the value ($3.5 \cdot 10^{-9}$ cm^2/s) of the pure polyimide [39], showing the marked effect of the rubbery phase content on average diffusivity rather than solubility. Moreover, we observe a dramatic increase of diffusivity above a certain PPO content, indicating a sharp transition from a glassy-like behavior to a rubbery-like behavior, that is also testified by changes of the shape of the trend line that best fits the mean solubility values. Such a transition is located between a PPO weight fraction of 43% and 59%. Corresponding charts obtained at 45 and 60°C show similar trends and are visible in the Supplementary Material in Fig. S3 and Fig. S4.

(a)

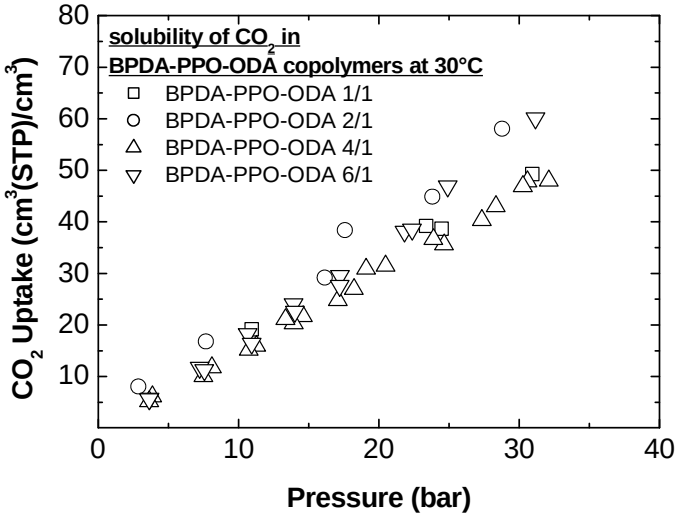

Fig. 5: The effect of copolymers composition on CO_2 solubility isotherms in BPDA-PPO4000-ODA copolymers at 30°C. Data at 45 and 60°C are reported in the Supplementary Material.

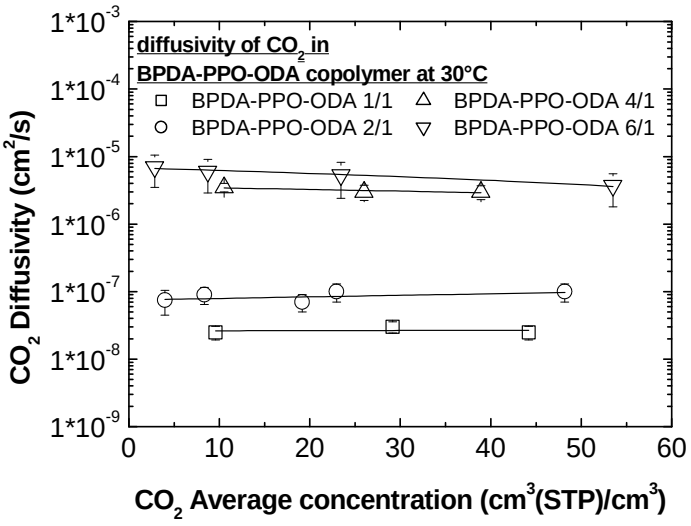

Fig.6: The effect of copolymers composition on CO_2 diffusivity in BPDA-PPO4000-ODA copolymers at 30°C. Solid lines are data interpolations. Data at 45 and 60°C are reported in the Supplementary Material.

2.2. Solubility and diffusivity of CO_2 in BKDA-PEO6000-ODA copolymers

As for the previous series of materials, also for this series we carried out sorption experiments in the temperature range 30-60 °C up to 30 bar to observe effects of operative conditions and copolymer compositions on solubility and diffusivity of CO_2. The solubility in these copolymers is lower than that observed in the copolymers based on PPO.

For BKDA-PEO-ODA 2/1 solubility decreases significantly going from 30°C to 45°C, after that a slight variation can be observed increasing the temperature up to 60°C. On the contrary for BKDA-PEO-ODA 4/1 a gradual decrease of solubility with temperature can be observed in Fig. 7. Diffusivity increases significantly with temperature in these membranes, as reported in Fig. 8, in particular by increasing temperature from 30°C to 60°C, D increases of one order of magnitude from $3 \cdot 10^{-8}$ cm^2/s up to $5 \cdot 10^{-7}$ cm^2/s in 2/1 sample, while in 4/1 sample it varies by almost 2 orders of magnitude, from $3 \cdot 10^{-8}$ cm^2/s up to 10^{-6} cm^2/s The diffusivity value increases with CO_2

concentration due to a penetrant induced swelling, which has been calculated through LF EoS and will be shown in a subsequent section.

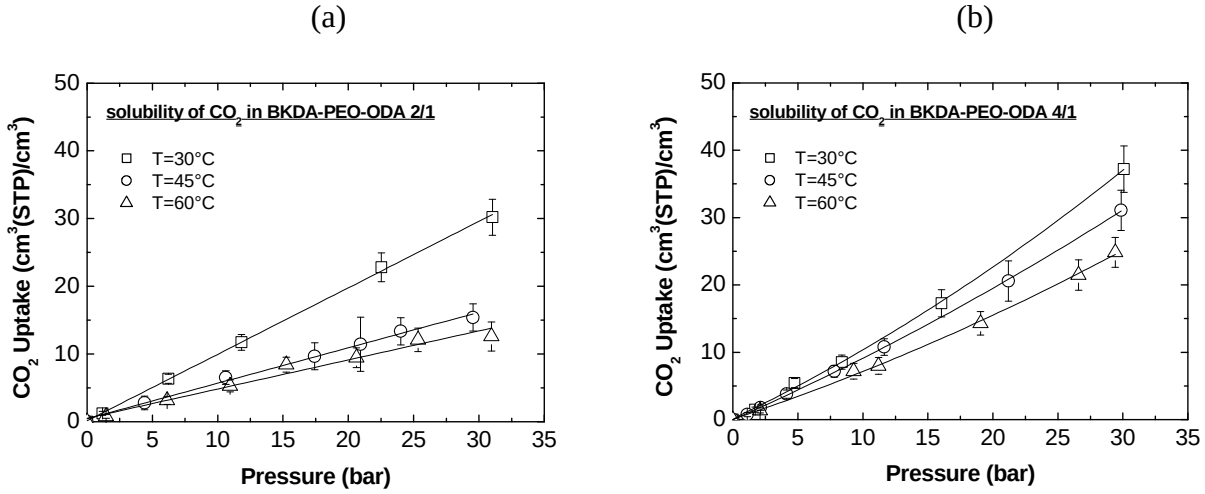

Fig.7: The effect of temperature on CO_2 solubility in BKDA-PEO6000-ODA 2/1 (a), 4/1 (b). Solid lines are data interpolations.

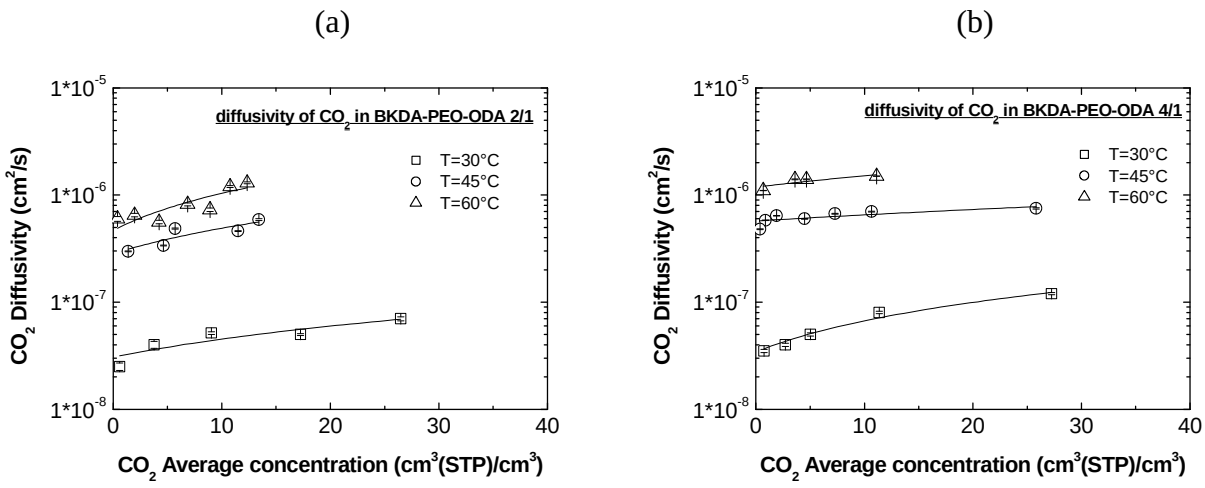

Fig.8: The effect of temperature on CO_2 diffusivity in BKDA-PEO6000-ODA 2/1 (a), 4/1 (b). Solid lines are data interpolations.

Considering the variation of CO_2 solubility with membrane composition, a higher effect of the rubbery PEO-phase than that observed for PPO-based copolymers is apparent from Fig. 9, that shows data at 30°C. By increasing PEO amount from 43.80 wt% to 60.40 wt% in the membrane [7-10], the solubility of CO_2 increases by 20% at 30°C, while at 45°C and 60°C solubility doubles (see the Supplementary Material, Fig. S5 and Fig. S6, for data at 45 and 60°C). Moreover, the solubility isotherms of these copolymers are never concave to pressure axis, as in the case of

glassy polymers, indicating a strong effect of the PEO-based rubbery phase over the glassy one, due also to higher proportions of rubbery phase used in these copolymers.

The CO_2 diffusivity at 30°C, reported in Fig. 10, increases by increasing PEO content in the membrane, although not as much as in PPO-based copolymers. In particular, all the PEO-based samples inspected have a mass fraction of PEO higher than 44 wt%, which is close to the threshold above which the PPO-based copolymers show a marked diffusivity increase. Similar trends are observed at 45 and 60°C, and are reported in the Supplementary Material in Fig. S7 and Fig. S8.

Therefore in this case, the observed increase of permeability with increasing PEO content in the membrane reported in previous works [7-10] is due to a simultaneous increase of solubility and diffusivity induced by the rubbery part of copolymer.

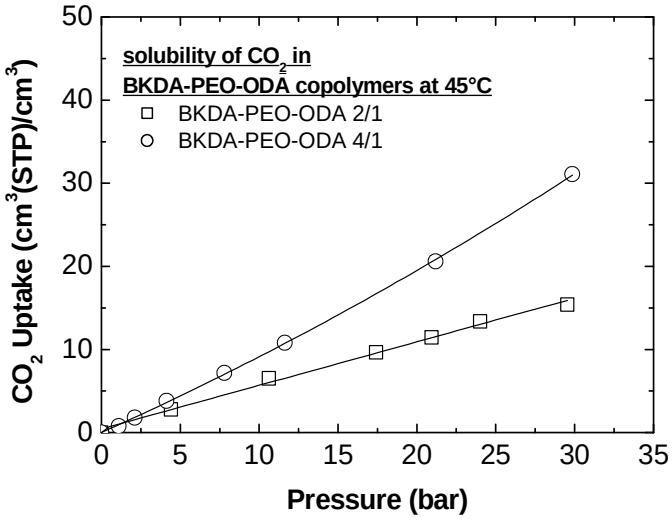

Fig.9: The effect of copolymers composition on CO_2 solubility isotherms in BKDA-PEO6000-ODA copolymers at 45°C. Solid lines are data interpolations. Data at 45 and 60°C are reported in the Supplementary Material.

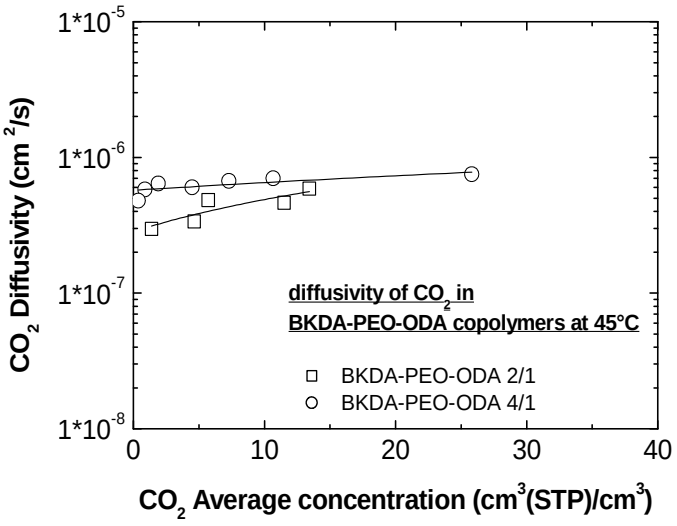

Fig. 10: The effect of copolymers composition on CO_2 diffusivity in BKDA-PEO6000-ODA copolymers at 45°C. Solid lines are data interpolations. Data at 45 and 60°C are reported in the Supplementary Material.

2.3. Sorption enthalpies and activation energies

The experimental data indicate that gas solubility decreases with increasing temperature in both series of copolymers, consistently with the exothermic nature of sorption. The composition of copolymers, however, affects the absolute value of the heat of absorption and consequently the dependence of solubility on temperature, as it can be seen in Fig. 11. For these materials, the sorption enthalpies increase in absolute value by increasing glassy phase content in the material, which is consistent with the higher values of sorption enthalpies normally observed in glassy phases. The values obtained are also in line with pure homopolymer values for BPDA-ODA [41], PPO [46] and PEO [47]. The sorption enthalpy is the sum of condensation and mixing effects: in the charts we provided, as an indication, the condensation enthalpy of CO_2, as a horizontal line, [48] so that the distance of total sorption enthalpy from this line quantifies the heat of mixing. The absolute values of sorption enthalpy decrease with increasing amount of rubbery phase on both set of copolyimides, falling approximately between the extreme values given by the sorption enthalpies of CO_2 in the two pure homopolymers. Glassy polymers are usually characterized by higher absolute values of gas sorption enthalpy with respect to rubbery polymers, due to the

presence of the additional free volume in the glassy state, which does not require the positive deformation energy to accommodate sorbed molecules. However, CO_2 sorption in rubbery polyethers is somehow peculiar because CO_2 interacts favorably with the polymer chain, giving rise to negative mixing enthalpies, that sum with the condensation enthalpy of CO_2 and produce sorption enthalpy values which are generally higher, in absolute values, than those measured for CO_2 in non polar rubbers.

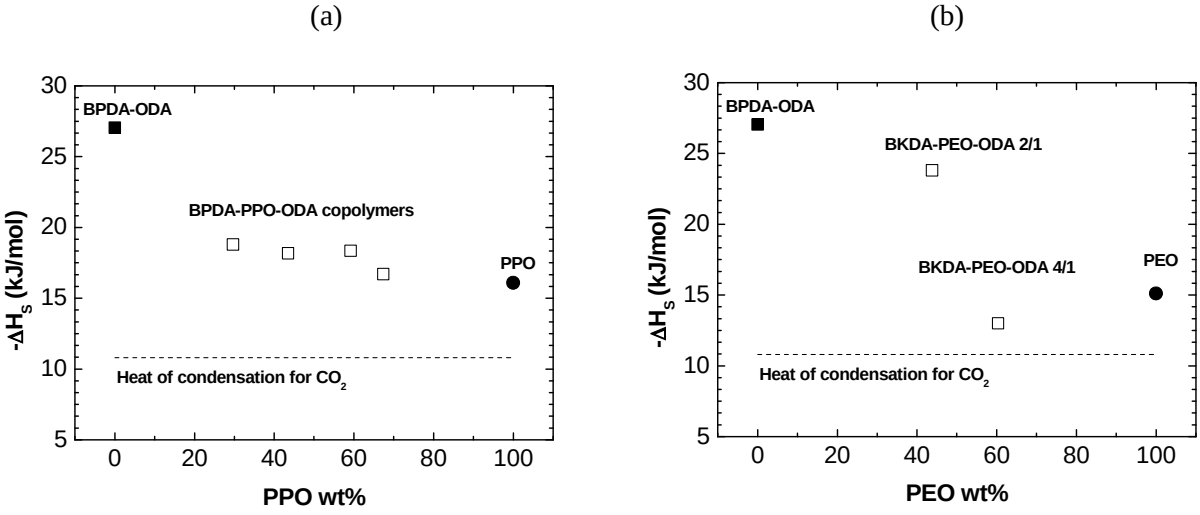

Fig.11: The effect of copolymers composition on CO_2 sorption enthalpies in BPDA-PPO-ODA (a) and BKDA-PEO-ODA (b) copolymers. Data of pure BPDA-ODA, PPO and PEO are taken from literature references [41], [46], [47].

For PPO copolymers, diffusivities follow an Arrhenius type of behavior in the entire range of temperature 30-60°C; on the contrary, for PEO copolymers a transition seems to occur between 35 and 45°C, which is consistent with data of permeability versus temperature reported in ref [7].

Activation energies for diffusion process in both series of copolymers are reported in Fig. 12.

The value of E_D measured in PEO copolymers, is at least double than the corresponding values measured in PPO copolymers at fixed CO_2 concentration. This difference may be related to the different glass transition temperature of the polyethers (203 K for PPO [6] and 250 K for PEO [49]): according to van Krevelen [50] the value of E_D for rubbery polymers increases with their T_g, while glassy polymers show the opposite behavior. For PPO copolymers, E_D decreases with increasing rubbery phase content, consistently with the fact that the rubbery phase is more flexible and mobile than the glassy one. On the other hand, in PEO-based copolymers the behavior with

composition is reversed; however, it must be said that in such case the error can be rather high, and that the crystalline content of the copolymer may increase with the amount of PEO, giving rise to higher energetic barrier for diffusion. For crosslinked PEO a value equal to 52 kJ/mol has been reported [51], while no value for pure PPO or BKDA-ODA is available.

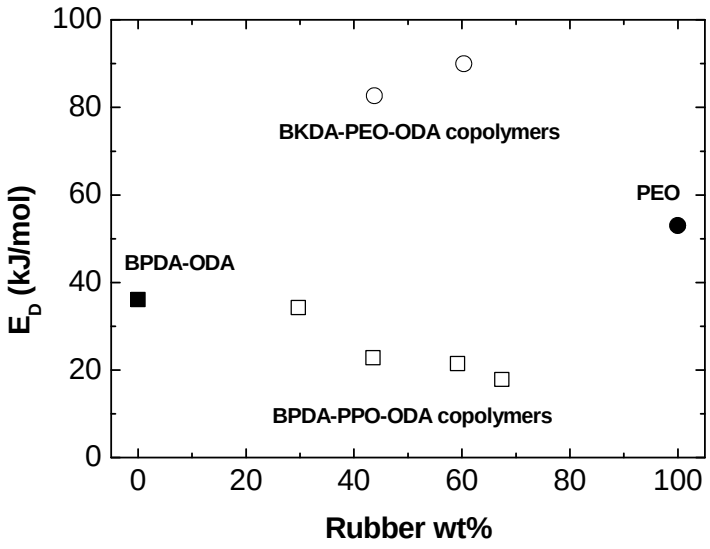

Fig.12: Activation energy for diffusion in BPDA-PPO-ODA and BKDA-PEO-ODA copolymers.

3. Models

The solubility of a gas in a rubbery or glassy polymer can be modelled and predicted with lattice fluid models, considering equilibrium and non-equilibrium conditions respectively, applying the equality of chemical potential of penetrant between the gaseous and the polymeric phase [13,25,26].

The LF models require knowledge of the pure components characteristic parameters, T^*, p^*, ρ^*, of polymers and penetrants, which can be obtained from best fit of LF EoS with vapor-liquid equilibrium data for gases and PVT data for polymers.

We report in Supplementary Material a table with the main equations and parameters of lattice fluid models.

The models also contain a binary gas-polymer interaction parameter, k_{ij}, which affects the characteristic pressure of the gas-polymer mixture and can be set equal to zero, in first order approximation, or adjusted on solubility data, and a swelling coefficient, $k_{sw,}$ that relates density to pressure and dry polymer density ρ_{POL}^{0} according to the following equation:

$$\rho_{POL} = \rho_{POL}^{0}(1 - k_{sw} p) \quad (7)$$

based on the experimentally observed gas-induced polymer dilation data [52-55]. The NELF model has been used to describe and even predict the solubility of pure and mixed fluids in many complex polymeric systems such as polymer blends, crosslinked polymers [27], semicrystalline structures [30] and composite materials [56-57]. In the present case we deal with a copolymer formed by a rubbery phase, at equilibrium, and a glassy phase, that is not at equilibrium. In general, both phases are active during the sorption process and the gas concentration can be expressed assuming additivity of the solubility contributions due to both phases, named c_R and c_G respectively:

$$c_{copol} = w_R c_R + (1 - w_R) c_R \quad (8)$$

In the above equation, the concentration of gas absorbed by the rubbery phase is estimated at each pressure with the LF EoS model, while the concentration of gas absorbed by the glassy phase is estimated with the NELF model. Different assumptions can be made for the degree of interaction and interpenetration between the two phases, which affect the choice of the parameters required by the equilibrium and non-equilibrium models in order to calculate the solubility.

In particular, use of the LF EoS to calculate the concentration of a gas dissolved in a rubbery polymer requires the values of the pure gas and pure polymer parameters, as recalled above, and of a binary energetic parameter k_{ij} (gas-polymer). In this work, we assumed that the rubbery pure polymer phase parameters are equal to those obtained for the corresponding pure rubbery homopolymer. The binary parameter k_{ij} is taken equal to the one obtained based on the solubility of the gas in the pure homopolymer.

Considering the density values of the polymeric phases to be used in the modeling, one has to account for the fact that the copolymer volume is lower than the sum of the homopolymer volume contributions, due to the negative mixing volume observed experimentally; thus the density of one or both phases is higher than that of the corresponding pure homopolymer. Indeed the glassy phase, by nature, can assume rather different density values at fixed pressure, temperature, and gas composition; however, also the rubbery phase present in the copolymer may be not free to assume the pure homopolymer equilibrium density value, due to the confinement by the rigid phase, reducing in such a way sorption capacity and diffusivity of penetrants in the polyether phase and resulting in lower solubility and diffusivity coefficients. In order to reduce the number of adjustable parameters in the model, and following physical considerations and model assumptions, we attributed the negative mixing volume entirely to the glassy phase, and assumed that the rubbery density value is equal to that of the pure homopolymer $\hat{v}_R = \hat{v}_R^0$. The glassy density value indeed is not a unique value because it can vary due to different sample histories; the NELF model is thus already set to account for such variations and to account for different values of polymer density, decoupled from the prevailing temperature, pressure and composition values. We were lead to this assumption also based on some previous results indicating that in these copolymers portions of the excess free volume of the glassy domains are penetrated by soft segments. Accordingly, the value of glassy specific volume in each copolymer, $\hat{v}_G$, can be calculated from experimental data of the copolymer volume with the following equation

$$\hat{v}_{copol} = w_R \hat{v}_R^0 + (1 - w_R)\hat{v}_G \qquad (9)$$

Such assumptions allow calculating solubility with a minimum number of experimental data as input, but can also provide a physical insight into the nature of the copolymers under consideration. In particular, the validity of the assumptions made on the density behavior of the copolymer material will be verified by comparing the calculation of the model with the experimental gas solubility data at different compositions. A good match will indicate that the

assumptions made about the interactions between rubbery and glassy phase are correct. As a further confirmation, we will also test the ability of alternative assumptions to represent the solubility data.

4. Modeling

4.1. Evaluation of pure component parameters

The lattice fluid pure component parameters, T^*, p^*, ρ^*, are required for CO_2 and for the different polymeric materials forming the copolymer. For the pure homopolymer PPO, no parameters were already available in the literature and we fitted the LF EoS model on the experimental Pressure-Volume-Temperature data. The fitting is reported in the Supplementary Material in Fig. S9; the maximum error between model and data is below 1% and the LF parameters obtained are listed in Table 2.

For BPDA-ODA and BKDA-ODA, pure component PVT data above T_g are not available and we followed a different procedure, as follows: the NELF model is fitted on experimental solubility data in the two pure glassy homopolymers, taken from the literature, at fixed pressure and temperature [18,25]. The fitting is carried out by keeping fixed and equal to zero the values of binary interaction parameters k_{ij} and swelling coefficients k_{sw}. The fitting between model and data is shown in the Supplementary Material in Fig. S10, and the set of parameters thus obtained is listed in Table 2, together with those of PPO, CO_2 and PEO taken from refs. [25] and [27], respectively.

Table 2: Sanchez and Lacombe pure component LF parameters

Component	T*	p*	ρ*	Reference	Source of data
	K	MPa	g/cm^3		
PPO	542	420	1.096	This work	[38] (PVT data)
PEO	590	620	1.218	[27]	
BPDA-ODA	570	480	1.610	This work	[41] (solubility of CO_2, CH_4, CO, H_2, N_2)
BKDA-ODA	670	600	1.530	This work	[40] (solubility of CO_2,

					CH_4, CO, O_2, N_2)
CO_2	300	630	1.515	[25]	

4.2. Evaluation of binary parameters

The binary parameters of the LF and NELF models have been fitted based on experimental data of CO_2 sorption or dilation in the pure homopolymers. For rubbery phases, which are in thermodynamic equilibrium, the only binary parameter is k_{ij}, while k_{sw} does not need to be specified, as it is a result of the model simulation itself being obtained from the equation of state for the gas-polymer mixture at that concentration. For glassy phases one needs to estimate also k_{sw}. A rather simple set of binary parameters has been used for the present modeling work:

-The binary interaction parameters k_{ij} are set equal to zero for all rubbery and glassy components, with the exception of those based on PEO, for which a value of k_{ij}=0.016 has been reported [30]. Such values allows to represent properly the CO_2 dilation data in the pure homopolymers PPO and PEO [46,47] (Figure 13 a, b), as can be seen in Figure 13 a and b, and were thus kept also for modeling the solubility of the components of the copolymer. Also the fitting of the solubility data in pure BPDA-ODA is adequate putting k_{ij}=0. (Figure 13 c, data from [39]) Such parameter represents interactions between CO_2 and monomers, and thus does not depend on the lengths of the polymeric components of the copolymers.

-The swelling coefficient has been set equal to zero (k_{sw}=0) for the glassy components, due to their rigidity. Such assumption also implies that only the rubbery phase is responsible for swelling of the copolymers, which can be estimated using the model. The assumption provides a good fit of the CO_2 solubility in pure BPDA-ODA taken from ref. [39] (Figure 13) and it was thus considered valid also for the BPDA-ODA phase present in the copolymers.

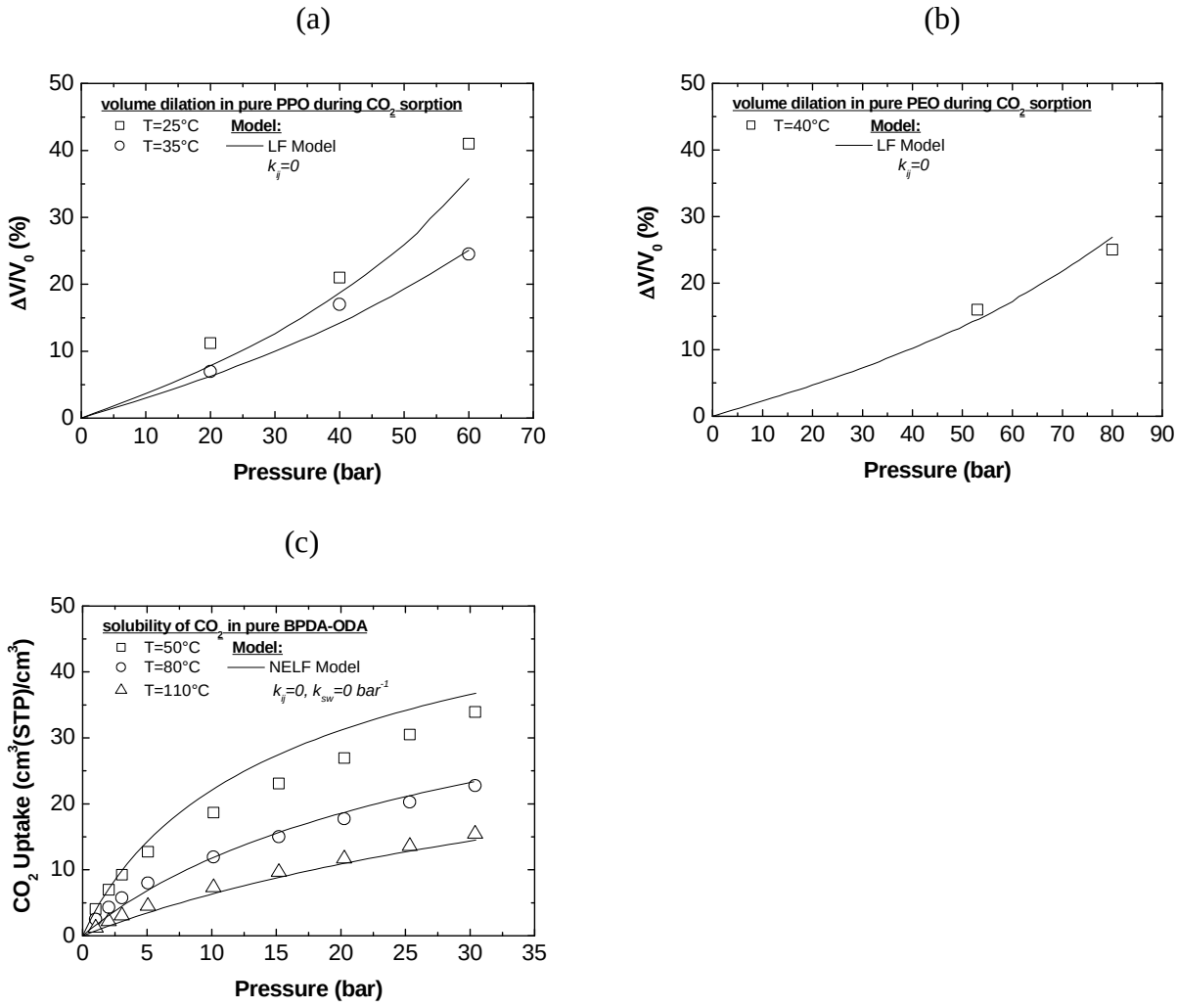

Fig.13: Comparison of LF model with experimental CO_2 -induced dilation in PPO (a) and PEO (b), and comparison of NELF model with solubility of CO_2 in BPDA-ODA (c) at different temperatures and pressures. Experimental data taken from ref. [46] (PPO), [47] (PEO), [39] BPDA-ODA.

4.3. Modeling CO_2 solubility in copolyetherimides

Using the proposed model with the reported values of the parameters, we obtain a good representation of the experimental data within the experimental error, as it can be seen in Fig. 14.

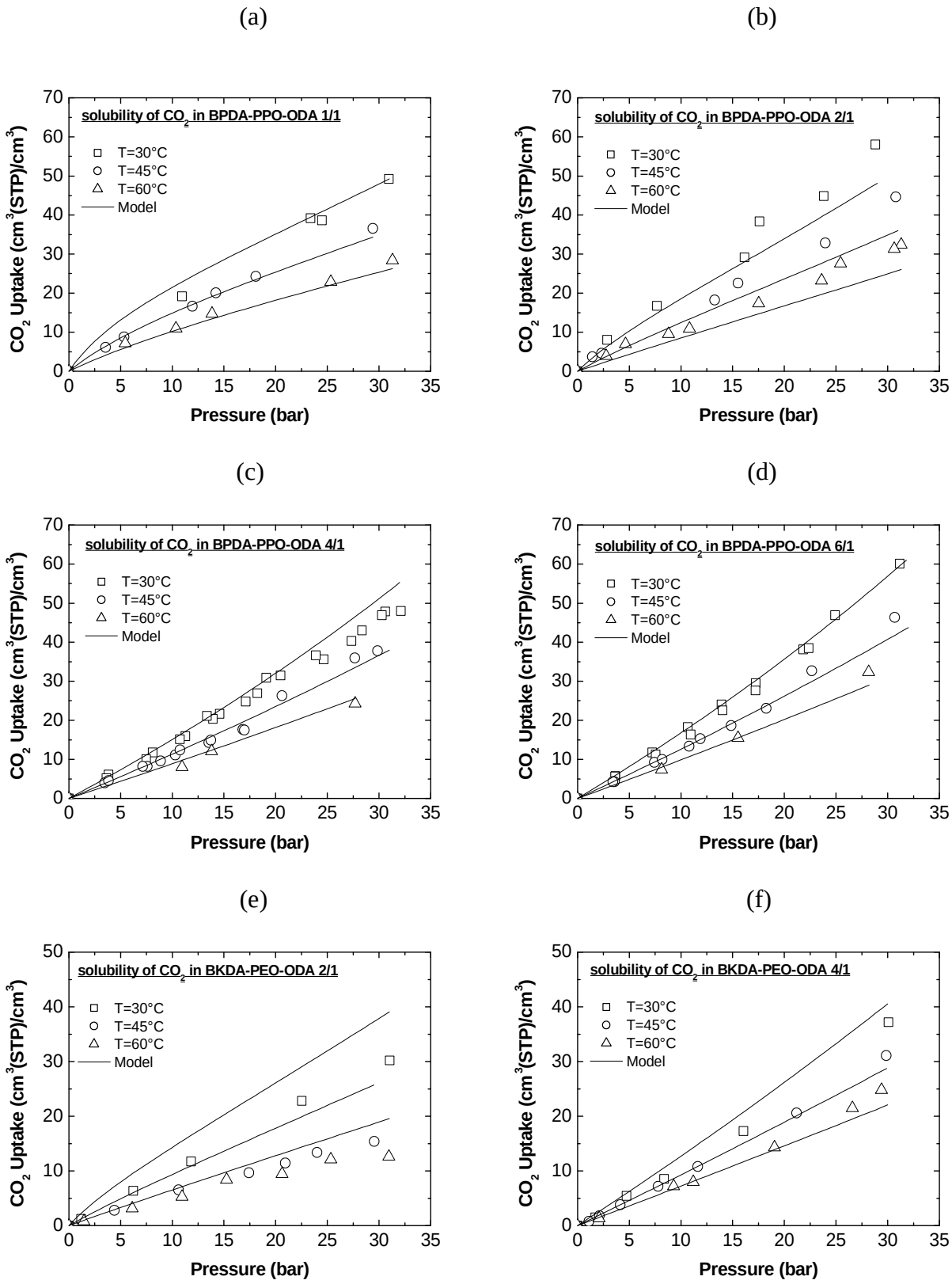

Fig. 14: Comparison between experimental solubility data and modelled solubility data with LF and NELF models in BPDA-PPO-ODA 1/1 (a), 2/1 (b), 4/1 (c), 6/1 (d) and BKDA-PEO-ODA 2/1 (e) and 4/1 (f) at 30°C, 45°C and 60°C.

It must be pointed out that no adjustable parameters were used in the model. The binary interaction parameters k_{ij} representing the energetic interactions between CO_2 and the two different phases are equal to those observed between CO_2 and the respective homopolymers, as it is reasonable, and are in almost all cases equal to the default value of zero. The same is true for swelling coefficient.

The good representation of solubility obtained with the model, at all compositions of the copolymers, confirms the validity of the approach followed and the set of parameters used, as well as the assumptions made on the physical behavior and structure of the copolymers. In particular, one notices that both phases contribute to gas sorption: the sorption capacity of the rubbery phase remains unvaried with respect to the one of the pure homopolymer, while that in the glassy phases decreases at increasing amounts of rubber in the copolymer, due to the reduction of free volume available for sorption. The model thus allows to conclude that the two phases form an interpenetrated structure, with the density and sorption capacity of the rubber equal to that of the pure polymer, and the density and sorption capacity of the glass moderately reduced by the presence of the rubber, which probably occupies part of its excess free volume, as discussed in the following.

The sensitivity of the model calculations to the assumptions and parameters used was tested in two different ways: first, we repeated the calculation of copolymer solubility considering the glassy polymer density equal to that of the pure homopolymer, parallel to what we did for the rubbery polymer. Such calculation shows that, although the solubility in the glassy phase is generally lower than that in the rubber, neglecting the glassy phase free volume reduction leads to a marked overestimation of copolymer solubility, as it is shown in the Supplementary Material in Fig. S11. Secondly, we attributed the deviation from additivity of the copolymer volume to both phases, i.e. we assumed that both the densities of the glassy and rubbery phases are varying as a function of copolymer composition, due to the presence of the second component. Indeed, if we consider the composite density data reported in Figure 2 as those of a simple liquid mixture, the partial molar volume of the two phases can be estimated with the intercept rule. Again, such calculations provide

a very poor fit of the solubility isotherms, and further support the conclusion that only the glassy phase, exhibits a volume contraction in the copolymer formation. The asymmetry of such behavior indicates that the specific volume reduction is not a consequence of a mechanism of compression and confinement exerted by one phase over the other, as such phenomenon would affect the volume of both phases to some extent. It is more likely, based on the data and the model analysis, that the excess free volume of the glass is partially occupied by the rubbery polyether segments. Such interpretation is also confirmed by the fact that the shape of the solubility isotherms of glassy-rich copolymers is closer to a linear behavior than to the typical concave one observed in glassy structures. Indeed the low pressure, non linear portion of the solubility isotherm of glassy polymers can be attributed to sorption into the excess free volume of the glass. A reduction of such excess free volume causes a reduction of the concavity, that is indeed observed in the present case and confirms the strong degree of interpenetration between the two phases in the copolymer.

4.4. Prediction of CO_2-induced swelling in copolyetherimides

According to previous work [20] and volume additivity equation (9), volume dilation during sorption in copoly(etherimides) can be predicted a priori as follows:

$$\frac{\Delta V}{V_0} = \frac{\omega_R \left(\left(\tilde{\rho}^R \rho^{*R} (1 - \omega_{CO_2}^R) \hat{v}_R^0 \right)^{-1} - 1 \right) \hat{v}_R^0 + \omega_G \left(\left(\tilde{\rho}^G \rho^{*G} (1 - \omega_{CO_2}^G) \hat{v}_G^0 \right)^{-1} - 1 \right) \hat{v}_G^0}{v_{copolymer}} \quad (10)$$

Where $\tilde{\rho}^R$, $\tilde{\rho}^G$, ρ^{*R}, ρ^{*G} are reduced densities and characteristic densities of rubbery and glassy phase during CO_2 sorption, respectively.

The values calculated are reported in Fig. 15 and show rather limited percentage swelling values, up to 10% for the PPO copolymers at the highest CO_2 pressure inspected. Such data indicate a certain robustness and resistance to plasticization of the matrix, even in the presence of high CO_2 pressures,

which can be problematic in the case of rubbery membranes. Coupled to the high CO_2 diffusivity (up to 10^{-5} cm^2/s) and permeability (around 10^2 Barrer) values measured in these copolymers, such data confirm the suitability of such materials for CO_2 capture applications, in a wide range of operative conditions.

In the presence of the rigid glassy domains the lower swelling of the rubbery phase with respect to the case of the pure homopolymers is also consistent with the shapes of the solubility isotherms of CO_2. It has been shown that such lines have a strong concavity towards the concentration axis in the pure polyethers (see for instance ref. [27]), even when they are crosslinked, as a consequence of a marked swelling induced by CO_2. In the case of the copolymers inspected here, on the other hand, such isotherms are almost linear, even in rubbery-rich copolymers, due to inhibition of swelling by the glassy phase, indicating a strong and beneficial interaction between the phases.

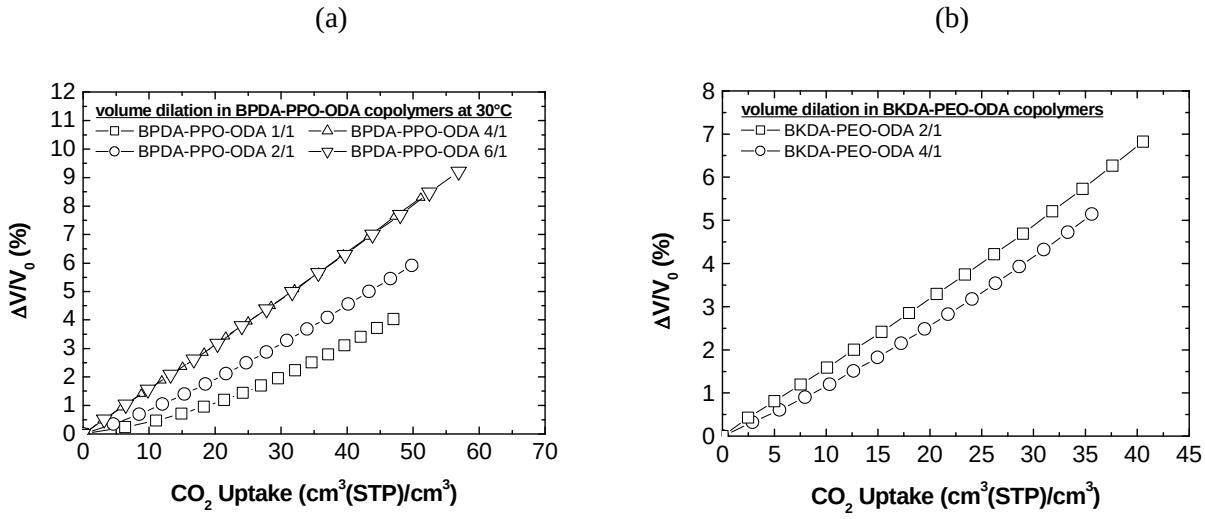

Fig. 15: Calculation of volume dilation in BPDA-PPO-ODA (a) and BKDA-PEO-ODA (b) at 30°C with LF model

5. Conclusions

The effects of temperature, pressure and copolymer composition on solubility and diffusivity of CO_2 have been studied in two series of copoly(ether-imides) made by hard (BPDA-ODA or BKDA-ODA) and soft (PPO or PEO) segments. In the case of BPDA-PPO-ODA copolymers the solubility is not dependent on copolymer composition, while, on the contrary, diffusivity strongly increases on

the rubbery phase content, due to higher mobility of PPO with respect to rigid BPDA-ODA. A dramatic increase of diffusivity is observed when the fraction of PPO is between 40 and 60 wt%, which can indicate a transition from a glassy-like to a rubbery-like behavior, as also indicated by the variation of the shape of the trendlines fitting the mean solubility values. On the other hand, in BKDA-PEO-ODA materials, which show a rubber-like behavior in almost all situations, both solubility and diffusivity increase by increasing PEO content in the membrane, due to the high affinity of CO_2 to the oxygen atoms of PEO. The effect of temperature has been studied both for solubility and diffusivity, obtaining sorption enthalpies and diffusion activation energy as a function of copolymer composition.

Finally, the NELF model was used to model CO_2 solubility in copolymers. In spite of its simplicity, the model proved accuracy in representing thermodynamic behavior of mixture formed by CO_2 and both series of copolymers. The success of the approach seems to confirm the physical assumptions underlying it, and in particular that both phases absorb CO_2; the rubbery phase maintains the same volumetric and sorption behavior as in the respective pure homopolymer, while the glassy phase volume is reduced by the presence of the rubbery phase, and consequently its ability to absorb CO_2 is also reduced. Such a behavior is attributed to the fact that the excess glassy free volume is partially occupied by the rubbery segments, and generally confirms the strong degree of interpenetration of such hybrid structure. The CO_2-induced swelling, estimated with the model, remains below 10%, due to the presence of the rigid glassy phase, even in samples in which the amount of rubbery phase is high: such behavior is due to the stabilizing presence of the glassy segments.

Acknowledgements

We acknowledge the financial support provided, by MINECO (MAT2011-25513, MAT2010-20668, MAT2013-45071-R and CTQ2012-31076).

References:

[1] C. H. Yu, C. H. Huang, C. S. Tan, A review of CO_2 capture by Absorption and Adsorption, Aerosol Air Qual. Res. 12 (2012) 745–769.
[2] J. K. Adewole, A. L. Ahmad, S. Ismail, C. P. Leo, Current challenges in membrane separation of CO_2 from natural gas: a review, Int. J. Greenh. Gas Control 17 (2013) 46–65.
[3] R. Bounaceur, N. Lape, D. Roizard, C. Vallieres, E. Favre, Membrane processes for post-combustion carbon dioxide capture: A parametric study, Energy 31 (2006) 2556–2570.
[4] L. M. Robeson, The upper bound revisited, J. Membr. Sci. 320 (2008) 390–400.
[5] H. Ohya, V. V. Kudryavtsev, S. I. Semenova, Polyimide Membranes - applications, fabrications and properties, Kodansha LTD and Gordon and Breach Science Publishers S. A., Japan, 1996.
[6] A. Tena, A. M. Fernandez, A. E. Lozano, J. C. De La Campa, J. de Abajo, L. Palacio, P. Pradanos, A. Hernandez, Thermally Segregated Copolymers with PPO Blocks for Nitrogen Removal from Natural Gas, Ind. Eng. Chem. Res 52 (2013) 4312–4322.
[7] A. Tena, A. E. Lozano, L. Palacio, A. M. Fernandez, P. Pradanos, J. de Abajo, A. Hernandez, Gas separation properties of systems with different amounts of long poly(ethylene oxide) segments for mixtures including carbon dioxide, Int. J. Greenh. Gas Control 12 (2013) 146–154.
[8] A. M. Fernandez, A. Tena, A. E. Lozano, J. G. de la Campa, J. de Abajo, L. Palacio, P. Prádanos, A. Hernández, Physical properties of films made of copoly(ether-imide)s with long poly(ethylene oxide) segments, Eur. Polym. J. 46 (2010) 2352-2364.
[9] A. Tena, A. Marcos Fernández, L. Palacio, P. Prádanos, A. E. Lozano, J. de Abajo, A. Hernández, On the influence of the proportion of PEO in thermally controlled phase segregation of copoly(ether-imide)s for gas separation, J. Membr. Sci. 434 (2013) 26–34.
[10] A. Tena, M. de la Viuda, L. Palacio, P. Prádanos, Á. M. Fernández, Á. E. Lozano and A. Hernández, Prediction of gas permeability of block-segregated polymeric membranes by an effective medium model, J. Membr. Sci. 453 (2014) 27–35.
[11] S. L. Liu, L. Shao, M. L. Chua, C. H. Lau, H. Wang, S. Quan, Recent progress in the design of advanced PEO-containing membranes for CO_2 removal, Prog. Polym. Sci. 38 (2013) 1089–1120.
[12] M. Yoshino, K. Ito, H. Kita, K-I Okamoto, Effects of hard-segment polymers on CO_2/N_2 gas separation properties of poly(ethylene oxide)-segmented copolymers, J. Polym. Sci. Part B, Polym. Phys. 38 (2000) 1707–1715.
[13] M. G. De Angelis, G. C. Sarti, Solubility of gases and liquids in Glassy Polymers, Annu. Rev. Chem. Biomolec. Eng. 2 (2011) 97–120.
[14] P. J. Flory, Thermodynamics of high polymer solutions, J. Chem. Phys. 9 (1941) 660–61
[15] M. L. Huggins, Solutions of long chain compounds, J. Chem. Phys. 9 (1941) 440.
[16] P. J. Flory, Thermodynamics of polymer solutions, Discuss. Faraday Soc. 49 (1970) 7–29.
[17] I.C. Sanchez, R.H. Lacombe, Statistical thermodynamics of polymer solution, Macromolecules 11 (1978) 1145–1156.
[18] S. H. Huang, M. Radosz, Equation of state for small, large, polydisperse, and associating molecules, Ind. Eng. Chem. Res. 29 (1990) 2284–94.
[19] T. Hino, J. M. Prausnitz, Perturbed hard-sphere-chain equation of state for normal fluids and polymers using the square-well potential of variable width, Fluid Phase Equilib., 138 (1997) 105–130.
[20] M. G. De Angelis, T. C. Merkel, V. I. Bondar, B. D. Freeman, F. Doghieri, G. C. Sarti, Hydrocarbon and Fluorocarbon Solubility and Dilation in Poly(dimethylsiloxane): Comparison of Experimental Data with Predictions of the Sanchez-Lacombe Equation of State, Journal of Polymer Science, Part B, Polymer Physics 37 (1999) 3011–3026.
[21] K. Nakanishi, H. Odani, M. Kurata, T. Masuda, T. Higashimura, Sorption of alcohol vapors in a di-substituted poly acetylene, Polym. J. 19 (1987), 293–304

[22] R. M. Barrer, J. A. Barrie, J. Slater, Sorption and diffusion in ethyl cellulose. Part III. Comparison between ethyl cellulose and rubber, J. Polym. Sci. 27 (1958) 177–197.
[23] A. S. Michaels, W. R. Vieth, J. A. Barrie, Solution of gases in polyethylene terephthalate. J. Appl. Phys. 34 (1963) 1–12.
[24] S. S. Jordan, W. J. Koros, A free volume distribution model of gas sorption and dilation in glassy polymers, Macromolecules 28 (1995) 2228–2235.
[25] G. C. Sarti, F. Doghieri, Nonequilibrium Lattice Fluids: A Predictive Model for the Solubility in Glassy Polymers, Macromolecules 29 (1996) 7885–7896.
[26] G. C. Sarti, F. Doghieri, Solubility of gases in glassy polymers based on the NELF model, Chemical Engineering Science 19 (1998) 3435–3447.
[27] M. Minelli, M. G. De Angelis, M. G. Baschetti, F. Doghieri, G. C. Sarti, C. P. Ribeiro, B. D. Freeman, Equation of State Modeling of the Solubility of CO_2/C_2H_6 Mixtures in Cross-Linked Poly(ethylene oxide), Ind. Eng. Chem. Res 54 (2015) 1142–1152.
[28] M. Minelli, G. Cocchi, L. Ansaloni, M. Giacinti Baschetti, M.G. De Angelis, F. Doghieri Vapor and Liquid Sorption in Matrimid Polyimide: Experimental Characterization and Modeling, Ind. Eng. Chem. Res 52 (2013), 8936-8945.
[29] M. Minelli, G.C. Sarti, Permeability and diffusivity of CO_2 in glassy polymers with and without plasticization, J. Membr. Sci. 435 (2013) 176-185.
[30] M. Minelli, M. G. De Angelis, An equation of state (EoS) based model for the fluid solubility in semicrystalline polymers, Fluid Phase Equilib.367 (2014) 173–181. [31] Meilchen, M. A. McHugh, Modeling High-Pressure Gas-Polymer Mixtures Using the Sanchez-Lacombe Equation of State, Journal of Applied Polymer Science 36 (1988) 583-597.
[32] I. C. Sanchez, P. A. Rodgers, Solubility of gases in polymers, Pure and Applied Chemistry 62 (1990) 2107-2114.
[33] Y. Sato, T. Takikawa, M. Yamane, S. Takishima, H. Masuoka, Solubility of carbon dioxide in PPO and PPO/PS blends, Fluid Phase Equilib.194–197 (2002) 847–858.
[34] E.M. Davis, Y.A. Elabd, Prediction of water solubility in glassy polymers using nonequilibrium thermodynamics, Ind. Eng. Chem. Res. 52 (2013) 12865-12875.
[35] Y. Lou, P. Hao, G. Lipscomb, NELF predictions of a solubility-solubility selectivity upper bound, J. Membr. Sci. 455 (2014) 247-253.
[36] F. Nilsson, K. Hallstensson, K. Johansson, Z. Umar, M. S. Hedenqvist, Predicting solubility and diffusivity of gases in polymers under high pressure: N_2 in polycarbonate and poly(ether-ether-ketone), Ind. Eng. Chem. Res, 52 (2013) 8655-8663.
[37] D.J. Branken, H. M. Krieg, G. Lachmann, P.A.B. Carstens, Modelling sorption and diffusion of NF3 and CF4 in Teflon AF perfluoropolymer membranes, J. Membr. Sci., 470 (2014) 294-306.
[38] P. Zoller, D. Walsh, Standard Pressure-Volume-Temperature Data for Polymers, Technomic, Lancaster, PA, 1995.
[39] K. Okamoto, K. Tanaka, H. Kita, A. Nakamura, Y. Kusuki, The effect of morphology on sorption and transport of carbon dioxide in a polyimide from 3,3′,4,4′-biphenyltetracarboxylic dianhydride and 4,4′-oxydianiline, Journal of Polymer Science 27 (1989) 1221–1233.
[40] K. Tanaka, H. Kita, M. Okano, K. Okamoto, Permeability and permselectivity in fluorinated and non-fluorinated polyimides, Polymer 33 (1992) 585–592.
[41] K. Tanaka, H. Kita, K. Okamoto, A. Nakamura, Y. Kusuki, Gas permeability and permselectivity in polyimides based on 3,3’,4,4’-Biphenyltetracarboxylic dianhydride, J. Membr. Sci. 47 (1989) 203–215.
[42] M. C. Ferrari, M. Galizia, M. G. De Angelis, G. C. Sarti, Gas and Vapor Transport in Mixed Matrix Membranes Based on Amorphous Teflon AF1600 and AF2400 and Fumed Silica, Ind. Eng. Chem. Res 49 (2010) 11920–11935.

[43] O. Vopicka, M. G. De Angelis, G. C. Sarti, Mixed gas sorption in glassy polymeric membranes: I. CO2/CH4 and n-C4/CH4 mixtures sorption in poly(1-trimethylsilyl-1-propyne) (PTMSP), J. Membr. Sci. 449 (2014) 97–108.
[44] J. Crank, The Mathematics of Diffusion, 2nd Ed., Oxford University Press, Oxford, 1975.
[45] T. C. Merkel, V. I. Bondar, K. Nagai, B. D. Freeman, I. Pinnau, 2000, Gas sorption, diffusion and permeation in Poly(dimethylsiloxane), Journal of Polymer Science Part B: Polymer Physics 38 (2000) 415–434.
[46] T. Guadagno, S. G. Kazarian, High-Pressure CO_2 Expanded Solvents: Simultaneous Measurement of CO_2 Sorption and Swelling of Liquid Polymers with in-Situ Near-IR Spectroscopy, J. Phys. Chem. B 108 (2004) 13995–13999.
[47] M. Hou, S. Liang, Z. Zhang, J. Song, T. Jiang, B. Han, Determination and modeling of solubility of CO_2 in PEG200 + 1-pentanol and PEG200 + 1-octanol mixtures, Fluid Phase Equilib. 258 (2000) 108–114.
[48] R. H. Perry, D. W. Green, Chemical Engineering Handbook, 7th Ed., Mc Graw Hill, New York, 1999.
[49] C. Wu, Simulated glass transition temperatures of Poly(ethylene oxide). Bulk and film: a comparative study, J. Phys. Chem. 115 (2011) 11044–11052.
[50] D. W. van Krevelen, K. te Nijenhuis, Properties of Polymers. Their correlation with chemical structure; their numerical estimation and prediction from additive group contribution, 4th Ed., Elsevier, 2009.
[51] C. P. Ribeiro Jr., B. D. Freeman, D. R. Paul, Pure and Mixed-gas Carbon Dioxide/Ethane Permeability and Diffusivity in a Cross-linked Poly(ethylene oxide) Copolymer, J. Membr. Sci. 377 (2011) 110–123.
[52] G. K. Fleming, W. J. Koros, Dilation of Polymers by Sorption of Carbon Dioxide at Elevated Pressures.1. Silicone Rubber and Unconditioned Polycarbonate, Macromolecules 19 (1986) 2285–2291.
[53] S. Jordan, W. J. Koros, Free volume distribution model of gas sorption and dilation in glassy polymers, Macromolecules 28 (1995) 2228–2235.
[54] M. G. De Angelis, T. C. Merkel, V. I. Bondar, B. D. Freeman, F. Doghieri, G. C. Sarti, Gas Sorption and Dilation in Poly(2,2-bistrifluoromethyl-4,5-difluoro-1,3-dioxole- co-tetrafluoroethylene): Comparison of Experimental Data with Predictions of the Nonequilibrium Lattice Fluid Model, Macromolecules 35 (2002) 1276–1288.
[55] V. Carlà, K. Wang, Y. Hussain, K. Efimenko, J. Genzer, C. Grant, G. C. Sarti, R. G. Carbonell, F. Doghieri, Nonequilibrium model for sorption and swelling of bulk glassy polymer films with supercritical carbon dioxide, Macromolecules 38 (2005) 10299–10313.
[56] M. Galizia, M. G. De Angelis, M. Messori, G. C. Sarti, Mass transport in hybrid PTMSP/Silica membranes, Ind. Eng. Chem. Res 53 (2014) 9243–9255.
[57] M. G. De Angelis, G. C. Sarti, Gas sorption and permeation in mixed matrix membranes based on glassy polymers and silica nanoparticles, Curr. Opin. Chem. Eng. 1 (2012) 148–155.

Supplementary Material

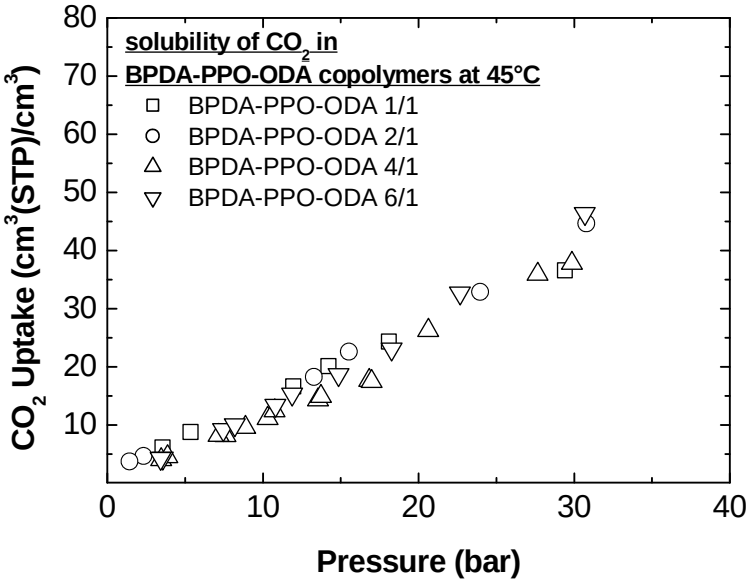

Fig. S1: The effect of copolymers composition on CO_2 solubility isotherms in BPDA-PPO4000-ODA copolymers at 45°C.

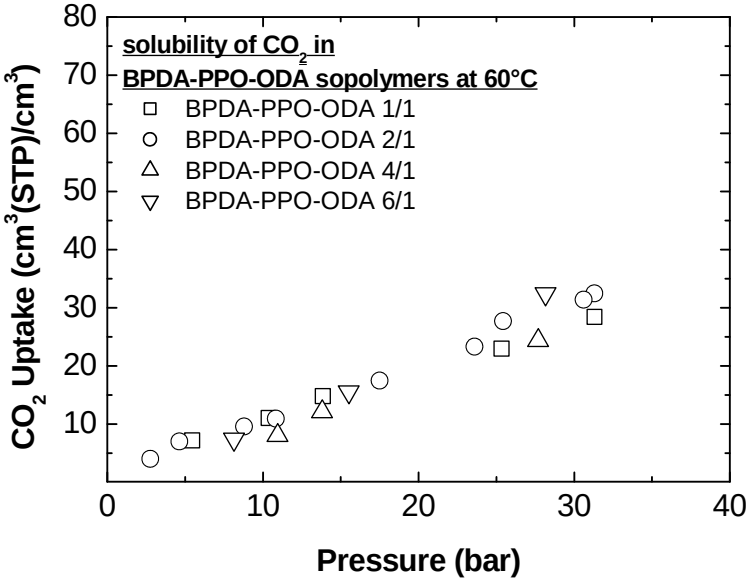

Fig. S2: The effect of copolymers composition on CO_2 solubility isotherms in BPDA-PPO4000-ODA copolymers at 60°C.

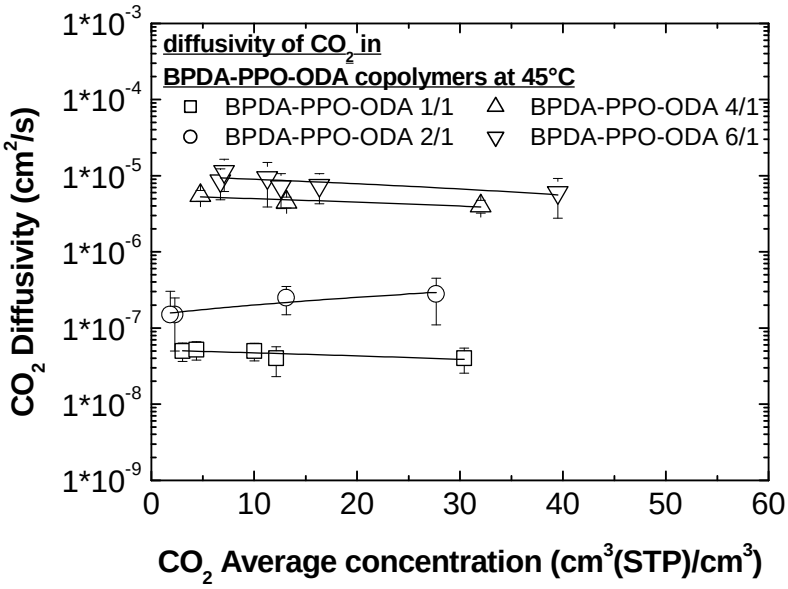

Fig. S3: The effect of copolymers composition on CO_2 diffusivity in BPDA-PPO4000-ODA copolymers at 45°C. Solid lines are data interpolations.

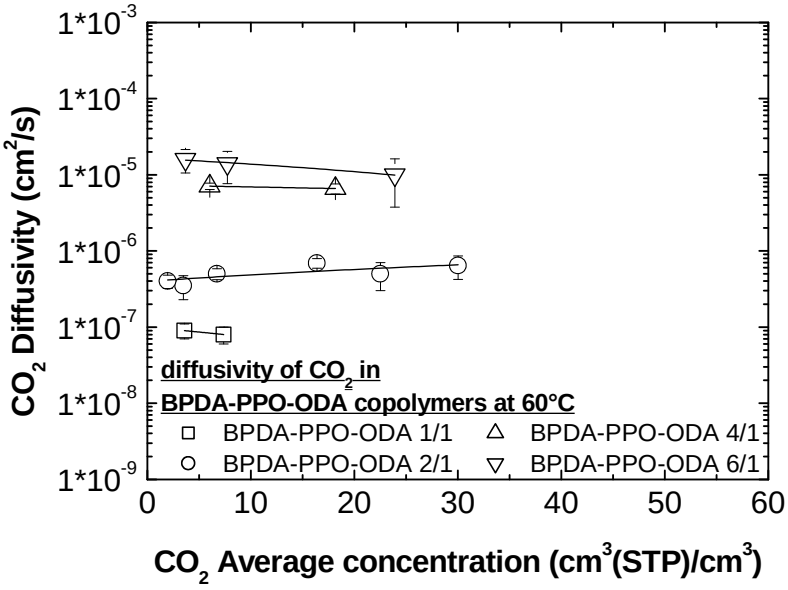

Fig. S4: The effect of copolymers composition on CO_2 diffusivity in BPDA-PPO4000-ODA copolymers at 60°C. Solid lines are data interpolations.

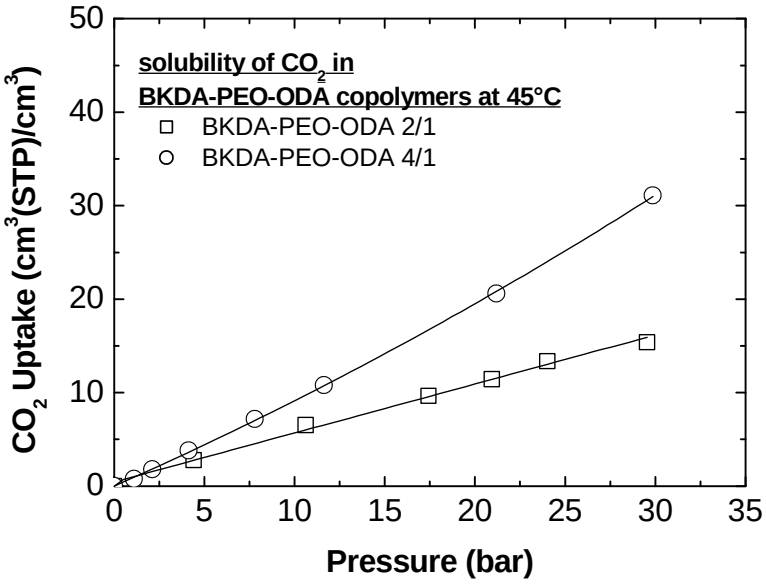

Fig. S5: The effect of copolymers composition on CO_2 solubility isotherms in BKDA-PEO6000-ODA copolymers at 45°C. Solid lines are data interpolations.

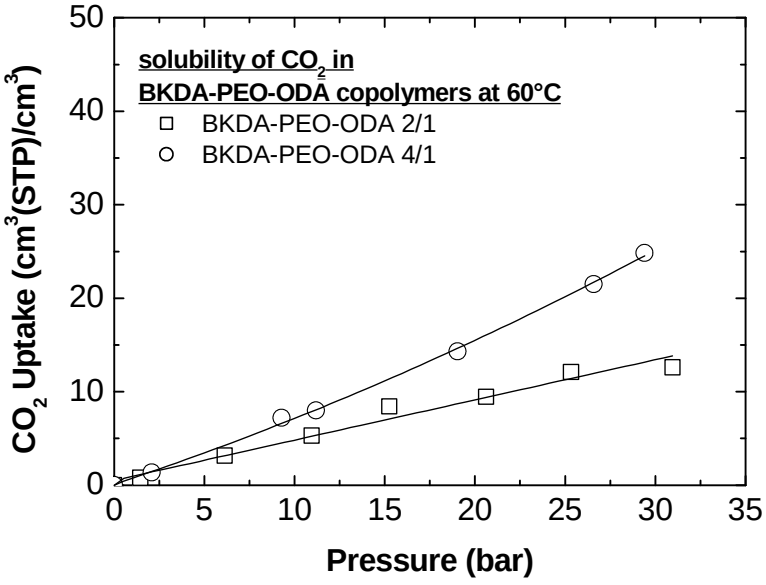

Fig. S6: The effect of copolymers composition on CO_2 solubility isotherms in BKDA-PEO6000-ODA copolymers at 60°C. Solid lines are data interpolations.

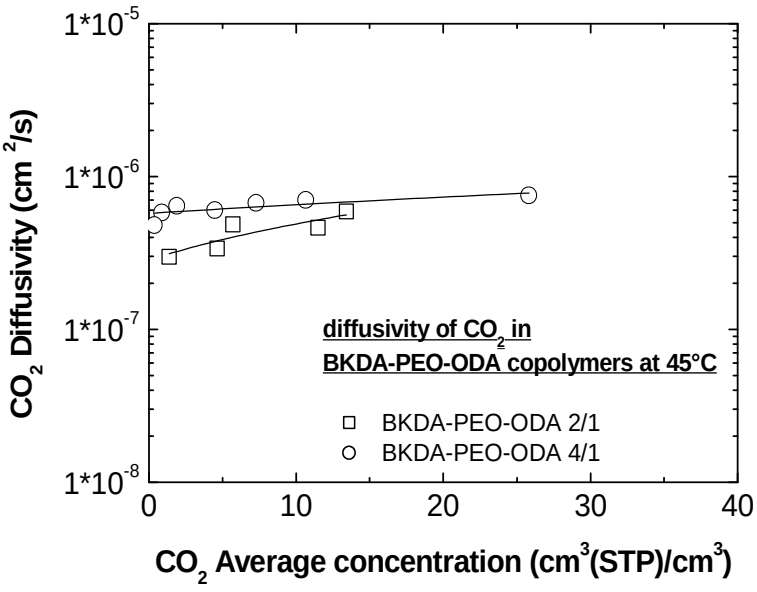

Fig. S7: The effect of copolymers composition on CO_2 diffusivity in BKDA-PEO6000-ODA copolymers at 45°C. Solid lines are data interpolations.

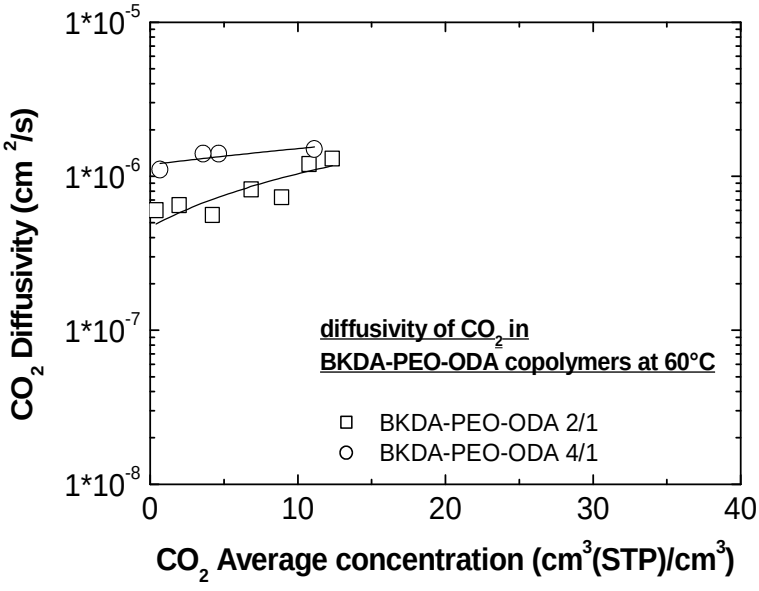

Fig. S8: The effect of copolymers composition on CO_2 diffusivity in BKDA-PEO6000-ODA copolymers at 60°C. Solid lines are data interpolations.

Table S1: Main equation of LF models

	Symbol	Name	Definition/property
Pure component i	ρ_i^*, p_i^*, T_i^*	Characteristic density, pressure and temperature	
	$\tilde{\rho}_i, \tilde{p}_i, \tilde{T}_i$	Reduced density, pressure and temperature	$\tilde{\rho}_i = \rho_i / \rho_i^*$; $\tilde{p}_i = p / p_i^*$; $\tilde{T}_i = T / T_i^*$
	v_i^*	Volume occupied by a mole of lattice sites	$v_i^* = \frac{RT_i^*}{p_i^*}$
	r_i^0	Number of lattice sites occupied by a molecule	$r_i^0 = \frac{M_i}{\rho_i^* v_i^*}$
	ω_i	Mass fraction	
	Φ_i	Volume fraction	$\Phi_i = \frac{\omega_i / \rho_i^*}{\sum_{i=1}^{N_p+1} \omega_i / \rho_i^*}$
Mixtures	ρ^*	Characteristic density	$1/\rho^* = \sum_{i=1}^{N_p+1} \omega_i / \rho_i^*$
	p^*	Characteristic pressure	$p^* = \sum_{i=1}^{N_p+1} \Phi_i p_i^* - \frac{1}{2} \sum_{i=1}^{N_p+1} \Phi_i \sum_{j \neq i} \Phi_j \Delta p_{ij}^*$
	Δp_{ij}^*	Binary parameter	$\Delta p_{ij}^* = p_i^* + p_j^* - 2(1 - k_{ij})\sqrt{p_i^* p_j^*}$
	k_{ij} , Ψ_{ij}	Binary parameter	$\Psi_{ij} = 1 - k_{ij}$
	r_i	Number of lattice sites occupied by a molecule	$r_i^0 v_i^* = r_i v^*$
	r	Molar average number of lattice sites occupied by a molecule	$r = \sum_{i=1}^{N_p+1} x_i r_i$
	T^*, v^*	Characteristic temperature, average close-packed mer molar volume	$T^* = \frac{p^*}{r} \sum_{i=1}^{N_p+1} x_i r_i^0 \frac{T_i^*}{p_i^*} = \frac{p^* v^*}{R}$

	$\tilde{\rho}, \tilde{p}, \tilde{T}$	Reduced density, pressure and temperature	$\tilde{\rho} = \rho / \rho^{*}$; $\tilde{p} = p / p^{*}$; $\tilde{T} = T / T^{*}$
		Equation of state for the fluid-polymer mixture (for pure *i*) $\Phi_i = 1$	$\tilde{\rho}^2 + \tilde{p} + \tilde{T}\left[\ln(1-\tilde{\rho}) + \tilde{\rho}\left(1 - \sum_{i=1}^{N_P+1} \frac{\Phi_i}{r_i}\right)\right] = 0$
	$\mu_i^{(S)}$	Chemical potential of *i* in the polymer mixture (for pure *i*) $\Phi_i = 1$	$\mu_i^{(S)} = \ln(\tilde{\rho}\Phi_i) - \ln(1-\tilde{\rho})(r_i^0 + (r_i - r_i^0)/\tilde{\rho}) + 1 - r_i - \tilde{\rho}\frac{r_i v_i^*}{RT}\left[p_i^* + \sum_{i=1}^{N_P+1} \Phi_i (p_i^* - \Delta p_{ij}^*)\right]$
	$\frac{\Delta V}{V_0}$	Volume dilation induced by penetrant sorption (V_0 is dry polymer volume)	$\frac{\Delta V}{V_0} = \frac{1}{\tilde{\rho}\rho^{*}(1-\omega_i)\hat{v}_{Polymer}^0} - 1$

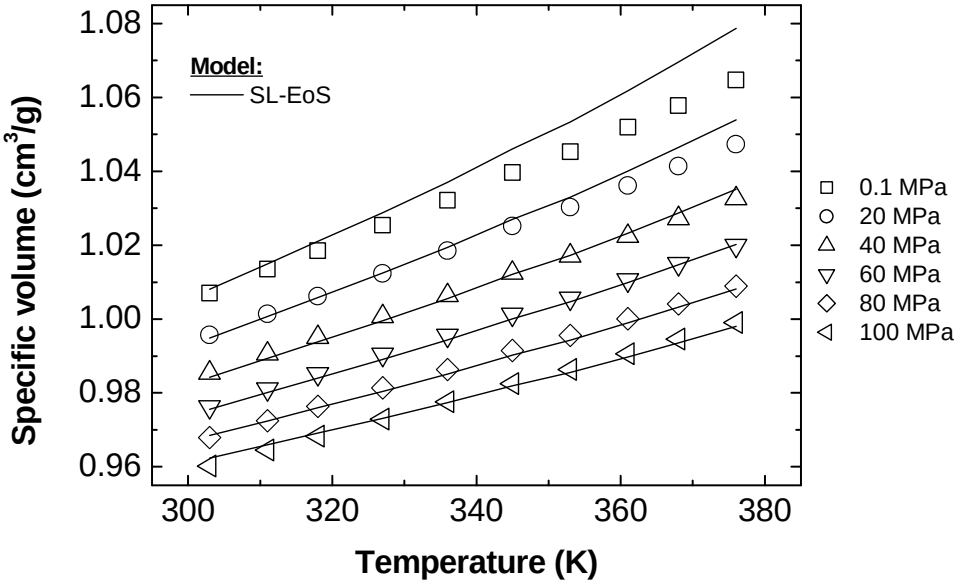

Fig. S9: Comparison of Sanchez and Lacombe LF-EoS and experimental data of specific volume of PPO at different temperature and pressure.

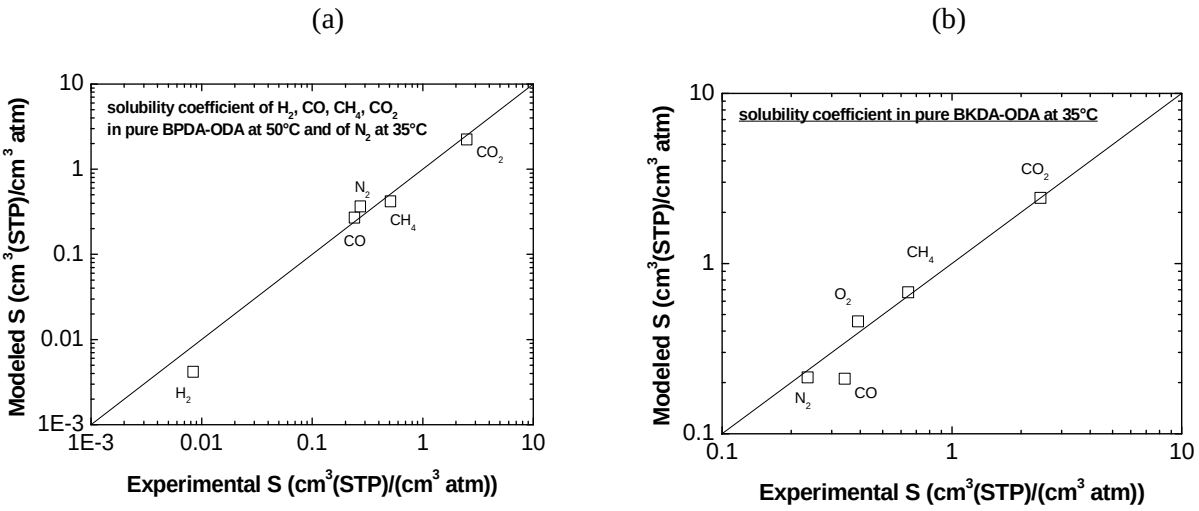

Fig. S10: Parity plot for comparison of NELF model and experimental solubility data in BPDA-ODA (a) and in BKDA-ODA (b). In particular for BPDA-ODA solubility coefficients are at 50°C and 10 atm [41] for H_2, CO, CH_4 and CO_2 and at 35°C and 2 atm for N_2 [40], while for BKDA-ODA data are at 35°C and 10 atm unless the case of N_2 and O_2, whose solubility coefficient is reported at 2 atm [40].

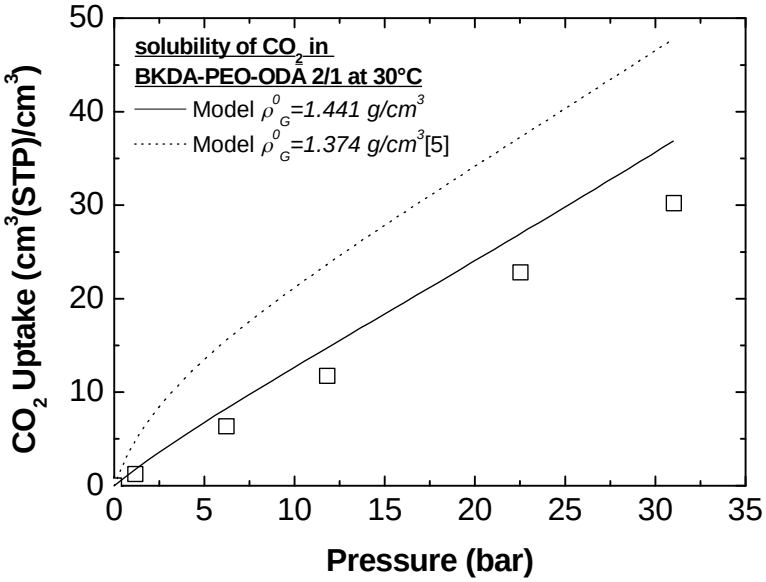

Fig. S11: Comparison of CO_2 solubility modeling results in BKDA-PEO-ODA 2/1 at 30°C with (solid line) and without (dashed line) density adjustment of glassy phase.

Table 2: Sanchez and Lacombe pure component LF parameters

Component	T*	p*	ρ*	Reference	Source of data
	K	**MPa**	**g/cm^3**		
PPO	542	420	1.096	This work	[38] (PVT data)
PEO	590	620	1.218	[27]	
BPDA-ODA	570	480	1.610	This work	[41] (solubility of CO_2, CH_4, CO, H_2, N_2)
BKDA-ODA	670	600	1.530	This work	[40] (solubility of CO_2, CH_4, CO, O_2, N_2)
CO_2	300	630	1.515	[25]	

Table 1: Properties of copolymer samples investigated in this work.

Sample	Rubber content	Amorphous rubber content	ρ	Thickness	Reference for density	Treatment temperature	T_g Rubber	T_g Glass
	wt%	wt%	g/cm^3	µm		°C	°C	°C
BPDA-PPO-ODA 1/1	29.70	29.70	1.267	161±19	Buoyancy method [6]	200	-71.6 [6]	240.1 [6]
BPDA-PPO-ODA 2/1	43.50	43.50	1.210	57±16	Buoyancy method [6]	160	-69.1[6]	225.7 [6]
BPDA-PPO-ODA 4/1	59.17	59.17	1.187	141±8	Interpolated, Equation 2	160	N/A	N/A
BPDA-PPO-ODA 6/1	67.38	67.38	1.159	154±43	Interpolated, Equation 2	160	N/A	N/A
BKDA-PEO-ODA 2/1	43.80	43.80	1.281	116±1	This work, weight and volume measurement	180	N/A	242 [8]
BKDA-PEO-ODA 4/1	60.40	59.90	1.244	107±2	This work, weight and volume measurement	180	N/A	189 [8]